



BRNO UNIVERSITY OF TECHNOLOGY

VYSOKÉ UČENÍ TECHNICKÉ V BRNĚ

FACULTY OF MECHANICAL ENGINEERING

FAKULTA STROJNÍHO INŽENÝRSTVÍ

INSTITUTE OF AEROSPACE ENGINEERING

LETECKÝ ÚSTAV

CONCEPTUAL STUDY OF GENERAL AVIATION ELECTRIC POWERED PLANE

KONCEPČNÍ NÁVRH LETOUNU GENERAL AVIATION NA ELEKTRICKÝ POHON

MASTER'S THESIS

DIPLOMOVÁ PRÁCE

AUTHOR

AUTOR PRÁCE

Iñigo Cervera

SUPERVISOR

VEDOUCÍ PRÁCE

Ing. Robert Popela, Ph.D.

BRNO 2023



Assignment Master's Thesis

Institut: Institute of Aerospace Engineering
Student: **Íñigo Cervera**
Degree program: Aerospace Technology
Branch: no specialisation
Supervisor: **Ing. Robert Popela, Ph.D.**
Academic year: 2022/23

As provided for by the Act No. 111/98 Coll. on higher education institutions and the BUT Study and Examination Regulations, the director of the Institute hereby assigns the following topic of Master's Thesis:

Conceptual study of general aviation electric powered plane

Brief Description:

Ecology in air transport is becoming more and more important in new aircraft designs. One of alternative ways is full or partial electrical power unit. Based on dynamic development in area of electromobility in general there is need for investigation of potential for implementation in general aviation segment.

Master's Thesis goals:

Conceptual design of electrically powered general aviation aircraft. Creation of aircraft specification, selection and detailed analysis of power unit, aerodynamic design and performance analysis, weight and balance analysis of concept, cost analysis, marketing study.

Recommended bibliography:

Gudmundsson, Snorri. (2022). General Aviation Aircraft Design - Applied Methods and Procedures (2nd Edition). Elsevier. Retrieved from

<https://app.knovel.com/hotlink/toc/id:kpGAADAM02/general-aviation-aircraft/general-aviation-aircraft>

Waller, Michael. (2018). Electrification of Civil Aircraft and the Evolution of Energy Storage. SAE International. Retrieved from

<https://app.knovel.com/hotlink/toc/id:kpECAEES01/electrification-civil/electrification-civil>

Deadline for submission Master's Thesis is given by the Schedule of the Academic year 2022/23

In Brno,

L. S

doc. Ing. Jaroslav Juračka, Ph.D.

Director of the Institute

doc. Ing. Jiří Hlinka, Ph.D.

FME dean

DECLARATION

I declare that I have written my master's thesis on the theme of "Conceptual study of general aviation electric powered plane" independently, under the guidance of the master's thesis supervisor and using the technical literature and other sources of information which are all quoted in the thesis and detailed in the list of literature at the end of the thesis. As the author of the master's thesis, I furthermore declare that, as regards the creation of this master's thesis, I have not infringed any copyright. In particular, I have not unlawfully encroached on anyone's personal and/or ownership rights and I am fully aware of the consequences in the case of breaking Regulation § 11 and the following of the Copyright Act No 121/2000 Sb., and of the rights related to intellectual property right and changes in some Acts (Intellectual Property Act) and formulated in later regulations, inclusive of the possible consequences resulting from the provisions of Criminal Act No 40/2009 Sb., Section 2, Head VI, Part 4.

Brno

.....
Author's Signature

Abstract

The design of electric aircraft represents an opportunity in the aviation field by offering promising advancements in terms of efficiency and sustainability. This project aims to explore the feasibility of designing a purely electric aircraft at a time when electric mobility is widespread in the automotive sector but not yet in the aviation industry. It will encompass the study of marketing and the market field, as well as the performance characteristics of the model, including the calculation of aircraft surfaces, with the goal of achieving the most realistic project possible.

Key words

Electric propulsion, Battery technology, Marketing, Weight analysis, Aircraft Performance, Glauert III, 3D Modelling, Catia V5.

INDEX

Abstract	5
Key words	5
1. Introduction.....	8
1.1 Aim of the design.....	8
1.1.1 Model overview (ELMIO M1)	9
.....	9
2. Market study	11
2.1 Target specifications.....	11
2.2 Identification of competitors.....	12
3. Surfaces design.....	15
3.1 Wing	15
3.1.1 Airfoil	16
3.1.2 Wing planform.....	16
3.1.3 Wing shape verification	18
3.2 Tail unit design.....	21
4. Propulsion unit	22
4.1 Engine selection.....	22
4.1.1 Emrax 208.....	22
4.1.2 Emrax 268.....	22
4.1.3 Emrax 228.....	23
4.2 Propeller selection.....	24
4.3 Battery selection.....	25
4.3.1 Charging time calculation	26
5. Structural design.....	28
6. Weight analysis.....	31
6.1 Component's weight estimation	31
6.2 Gravity centre estimation.....	35
7. Aircraft performance analysis	37
7.1.1 Wing drag estimation	37
7.1.3 Empennage drag estimation	40
7.1.4 Total drag.....	43

7.3	Power required and available	44
7.4	Maximum speed.....	46
7.5	Rate of climb.....	46
7.6	Operative ceiling.....	48
7.7	Range.....	49
7.8	Endurance.....	51
7.9	Take off distance	52
8.	Aircraft cost analysis.....	53
8.1	Workhours calculation	53
8.2	Costs calculation.....	53
8.3	Aircraft final price and break-even point	57
9.	Result comparison and conclusion.....	58
10.	References.....	59
11.	List of parameters.....	61

1. Introduction

1.1 Aim of the design

The transition to electric power for all vehicles has been well underway for some time now. As we look towards the future, there is a growing need to replace the aircraft that were designed and manufactured during the latter half of the previous century. Aircraft that have been a sale success such as the **Cessna 152** or the **Piper PA-28 Cherokee** which have sold 7 and 33 thousand units respectively will soon be in need of a replacement [1] [2].

In specific terms, our project focuses on the design of a two-seater full metal electric trainer aircraft that will meet the requirements of the CS-23 certification named **eLMIO M1**. This design could serve as the starting point for more complex models with a greater number of seats to expand in the market.

1.1.1 Model overview (eLMIO M1)

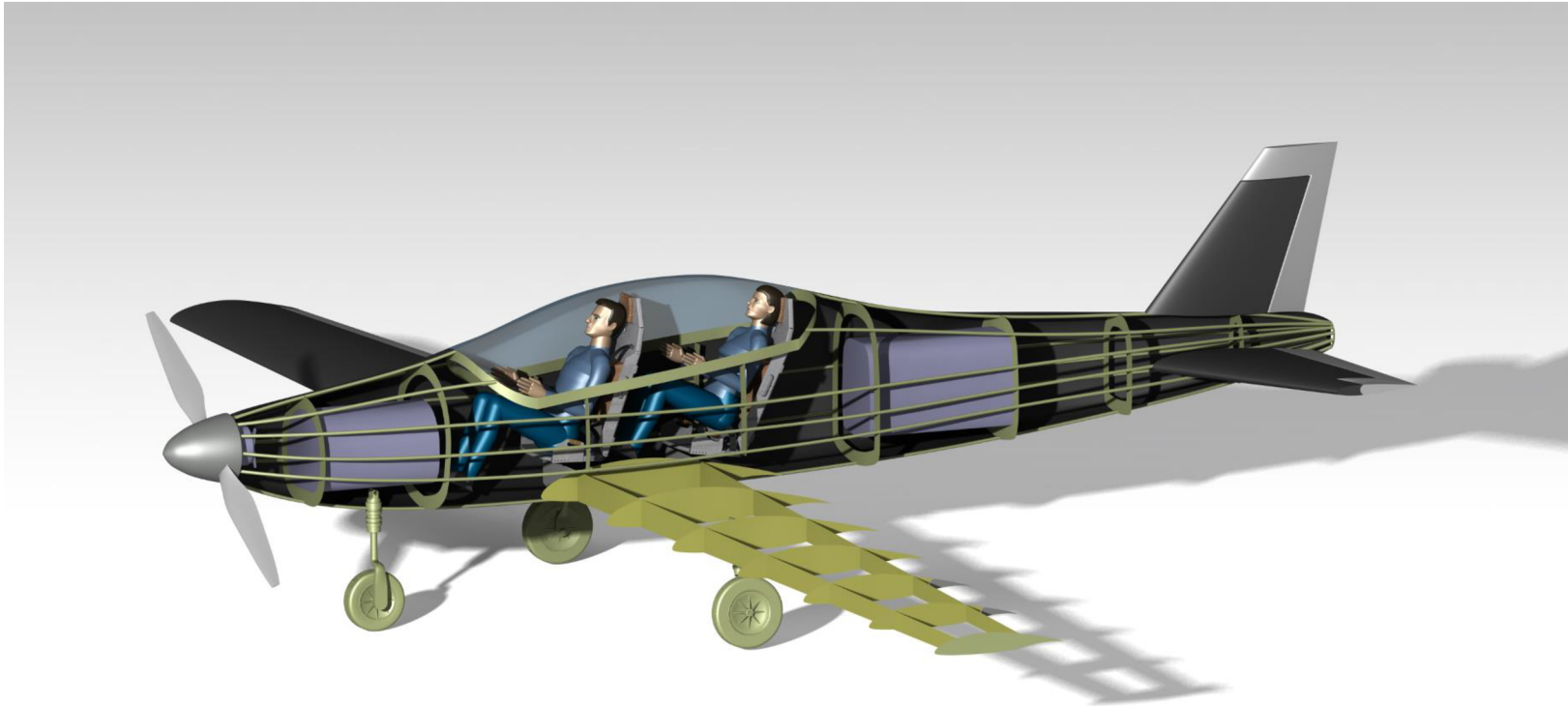


Figure 1.1 Model overview (CATIA).

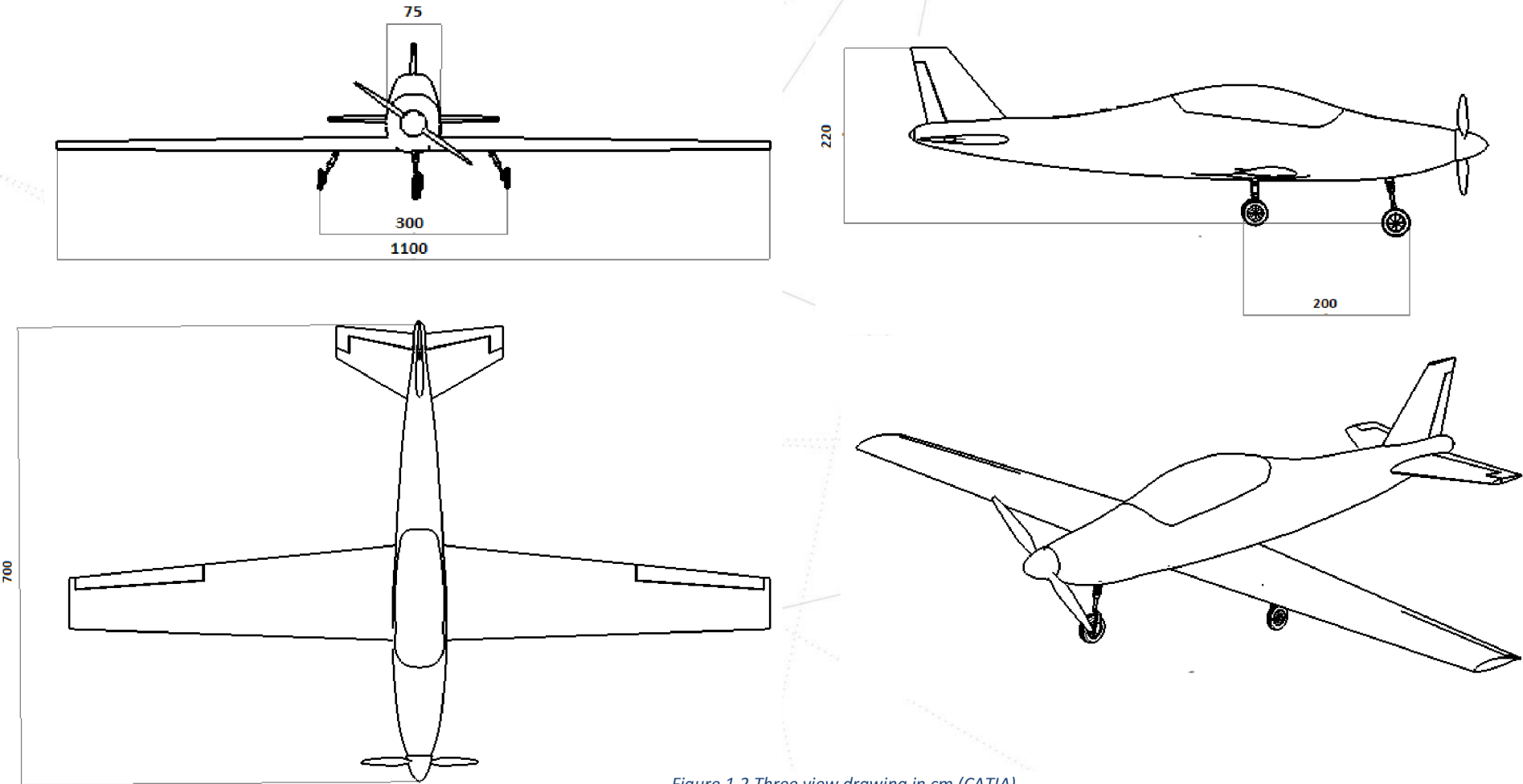


Figure 1.2 Three view drawing in cm (CATIA).

2. Market study

2.1 Target specifications

Given the design objective, our target specifications for the model will closely align with the specifications of the existing models we aim to replace. A comparison of the key features among the main models can be observed in the following table [1] [2]:

The wing size decision has been made through approximation, by comparing various models of aircraft with similar design purpose, and selecting a value close to the tendency line. It is important to mention that the list includes both electric and combustion powered aircraft.

The models compared:

- Piper Cherokee
- Cessna 152
- Diamond DA20 KATANA
- Liberty XL2
- Boomerang DW200
- Alpha 2000
- Piper PA17
- Pipistrel alpha electric
- Liaoning ruixiang XAE1
- Bye Aerospace Eflyer2
- Elmio M1
- Yuneec E430
- Beechcraft Skipper

For highlighting, our model is represented in red.

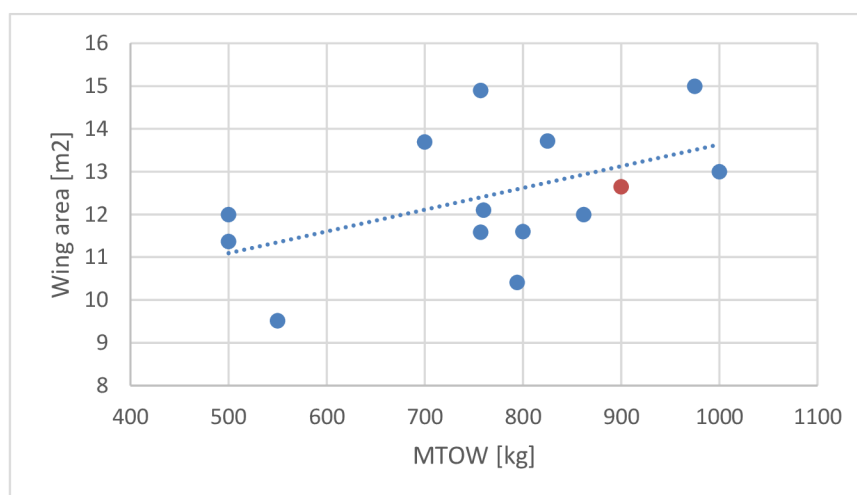


Figure 2.1 Ratio of wing area to MTOW for different models.

Same approach was followed for other specifications.

	PIPER CHEROKEE	CESSNA 152	ELMIO M1
Wingspan (m)	9,14	10,3	11
Wing area (m²)	15	14,9	12,65
Power plant	LYCOMING O320 E2A	LYCOMING O-235-L2C	*
Power (HP)	150	110	*
Power (kW)	110	82	*
MTOW (Kg)	975	757	900
V_{MAX} (km/h)	228	202	295
V_{CRUISE} (km/h)	200	123	235
V_{STALL} (km/h)	87	79	<110*
Range (km)	861	768	400
Endurance (h)	-	8,7	2
Units sold	32778	7584	NA
Aspect Ratio	5,569	7,120	9,565

*Given by regulation or not yet selected.

Table 2.1 Specification comparison between old models and target specifications.

2.2 Identification of competitors

Despite the fact that this sector of the market is relatively new, there are certain companies dedicating resources for the development of fully electric aircraft. Among them the following ones can be highlighted:

Pipistrel: Slovenian aircraft manufacturer established in 1989, ventured into the electric field around 2007 with the introduction of their Taurus Electro, the first fully electric two-seat aircraft to achieve serial production. Subsequently, they expanded their offerings by introducing a four-seat version of the same aircraft.

They have accomplished notable achievements, including participation in the HYPSTAIR program and developing the first four-seat passenger aircraft with zero emissions.

According to Pipistrel’s data, they have sold 2300 units of their aircraft by August of 2021.

In March 2022, Textron announced the acquisition of Pipistrel to establish a new division dedicated to electric aircraft development called Textron eAviation. This purchase was done for a total of 235 million USD [3].



Figure 2.2 Pipistrel’s logo [3].

Bye Aerospace: American aircraft manufacturer specialized on design and manufacture of electric aircraft, unmanned aircraft for geospatial role and light aircraft for training role. The first step was done in July 2010 when they developed a proof of concept electrically powered Cessna 172 in collaboration with Cessna Aircraft. By 2015, they furthered their progress by creating the Sun Flyer, a fully electric single-seat model that served as a prototype for the two-seat version known as the eFlyer 2. The eFlyer is specifically designed for the training flight market and features a single engine powered by Li-ion batteries [4].

This company will be the closest one we'll encounter in the market sector since, as t they develop their models with the same market target as ours [4].



Figure 2.3 Bye aerospace's logo [4].

Yuneec International: Originally a manufacturer of RC models, this Chinese aircraft manufacturer made a notable entry into the aviation industry by building the first successful electric-powered paraglider in serial production and by the manufacture of the Yuneec E430 aircraft. However, since 2014, the company has moved its focus towards the drone market [5].



Figure 2.4 Yuneec's logo [5].

In addition to these, a large number of companies are showing keen interest in electric aircraft and actively developing their own models, although these models have not been released yet.

Here we can see a comparison between the most interesting models from the previous named companies and ours:

	Pipistrel Alpha electro	Bye Aerospace eFLYER 2	Yuneec International E430	Elmio M1
Wingspan (m)	10,5	12	13,8	11
Wing area (m²)	9,51	12	11,37	12,65
Power plant	Pipistrel PEM 60MVLC	SAFRAN Emotor	Yuneec Power drive 40	N/A*
Power (HP)	80	135	54	N/A*
Power (kW)	60	101	40	N/A*
MTOW (Kg)	550	862	500	900
V_{MAX} (km/h)	194	250	150	295
V_{CRUISE} (km/h)	157	222	90	235
V_{STALL} (km/h)	Certif. Req	Certif. Req	Certif. Req	>111*
Range (km)	200	455	227	400
Endurance (h)	1	3,5	2,5	2
Units sold	500	NO DATA	NO DATA	N/A
Aspect Ratio	11,593	12	16,749	9,565

Table 2.2 Electric aircraft comparison.

3. Surfaces design

The design of the following areas has been calculated using the procedures outlined in the book *General Aviation Aircraft Design: Applied methods and procedures* [6].

3.1 Wing

The initial input values for the design include the wing area, maximum take-off weight, desired cruise speed, and the maximum stall speed, which is determined by CS23 regulations [6] [7].

$$V_{\text{STALL MAX}}=61 \text{ knots}$$

$$M_{\text{TOW}}=900 \text{ Kg}$$

$$V_{\text{CRUISE}}=235 \text{ Km/h}$$

$$\text{Wing Area}=12,65 \text{ m}^2$$

Wing loading will depend on the class of the aircraft. The most usual classes are represented in the following figure:

Aircraft Class	Typical Takeoff Wing Loading (Kg/m ²)
Sailplane	29
Homebuilt	54
General aviation – single engine	83
General aviation – twin engine	127
Twin turboprop	195
Jet trainer	244
Jet fighter	342
Jet transport / bomber	586
Super transporter / bomber	816

Figure 3.1 Typical wing loading [8].

With these values we can start the calculations:

$$\frac{M_{\text{tow}}}{A_{\text{min}}} = 83 \text{ kg/m}^2$$

This minimum area has to be lower than the value exposed at Table 2.2.

$$A_{\text{min}} = 10,84 \text{ m}^2$$

It is lower, so we can keep using the previous value.

Now let's compute the lift coefficient value for cruise conditions:

$$Cl(\text{aircraft}) = \frac{2M_{\text{tow}} * g}{\rho * V_{\text{cruise}}^2 * A} = 0.2673$$

$$Cl(\text{wing}) = 1,1 * Cl(\text{aircraft}) = 0.294$$

$$Cl(\text{airfoil}) = Cl(\text{wing})/0.85 = 0.356$$

Given the value of the lift coefficient (Cl), the objective is to find an airfoil that generates the least amount of drag for this particular lift coefficient.

3.1.1 Airfoil

In order to minimize drag and increase aerodynamic efficiency the selected airfoil belongs to the Natural Laminar Flow family of airfoils (NFL), this means that they are designed to maintain laminar flow over a bigger portion of the wing surface. (Kämpf, 2018)

For this particular scenario, the NLF (1) 0215 airfoil has been selected for the entire span of the aircraft's wings. Figure 3.2 illustrates the graphical representation of the lift, drag, and moment coefficients associated with this airfoil.

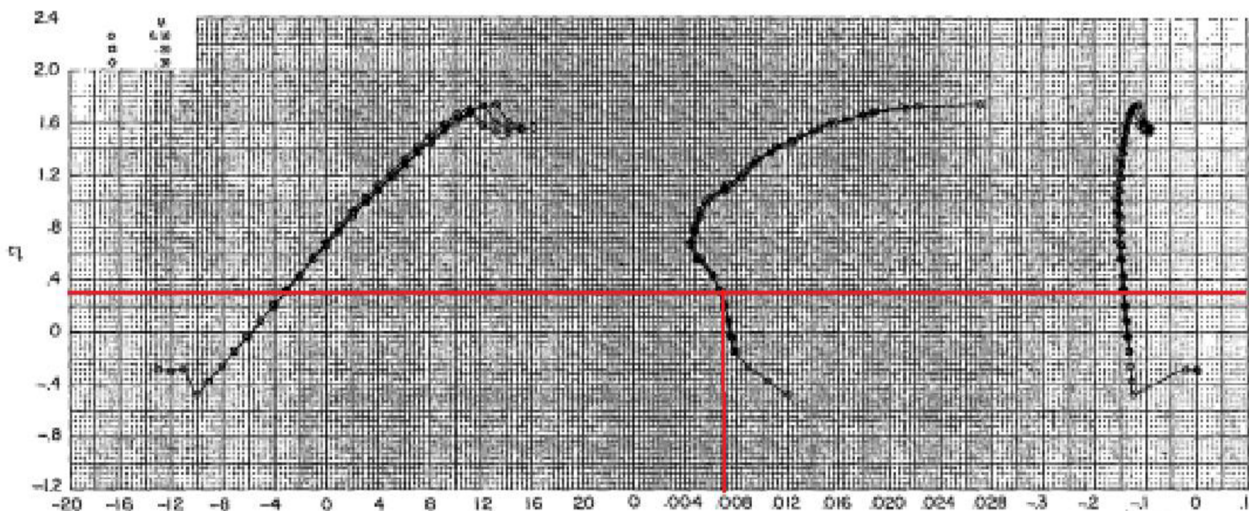


Figure 3.2 NLF (1) 0215 aerodynamic curves [9].

3.1.2 Wing planform

The wing shape is an important aspect in defining the aerodynamic characteristics of an aircraft. There are numerous shapes, each with its own advantages and disadvantages, which are applied based on the design objectives. In our case, it is required a wing shape that offers a good lift-to-drag ratio at low speeds without compromising maneuverability. The options that best fit this criterion are rectangular wing or tapered wing designs.

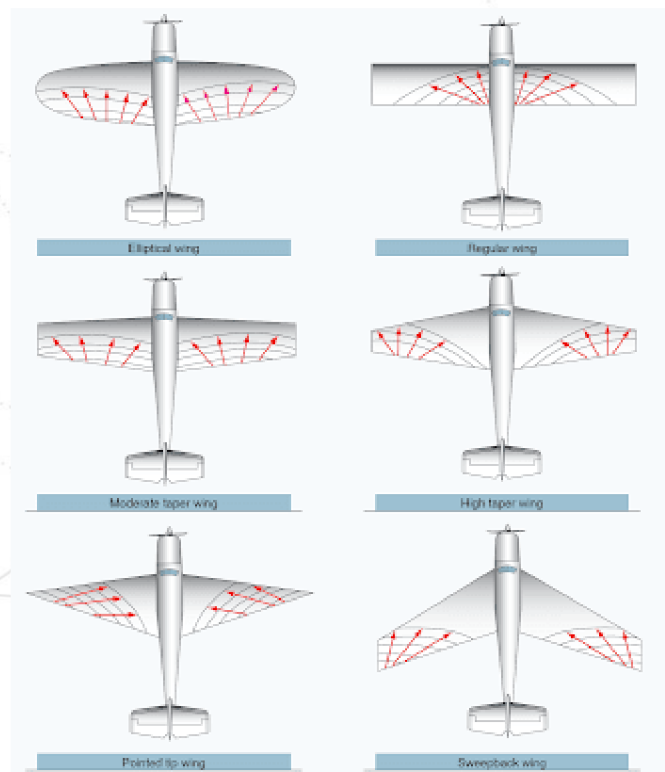


Figure 3.3 Different wing planforms [10].

On one hand, the rectangular wing is simpler to design and manufacture, and it offers good maneuverability at low speeds, going over the tapered wing in terms of roll rate. However, the rectangular wing has a higher weight, which is an important factor in this project. Additionally, it generates a higher drag, resulting in lower efficiency at higher speeds. These two characteristics have led me to choose the tapered wing shape.

Another important aspect of the planform design is the aspect ratio, which is the ratio of the square of the span to the wing area. This factor influences the structural integrity of the wings, maneuverability, parasite drag, and even the range (in the case of combustion aircraft with wing fuel tanks). Additionally, it is essential to consider the practicality of the aircraft's wingspan in relation to fitting into specific hangars. The higher the AR of the aircraft, the higher Lift/drag ratio will the wings have, however the aircraft will be less responsive in terms of maneuverability and less maximum speed will be achieved.

To make this decision, a slight sacrifice in wing efficiency has been made in order to achieve a higher speed than the competition specified in table 2.2.

The chosen wing geometry:

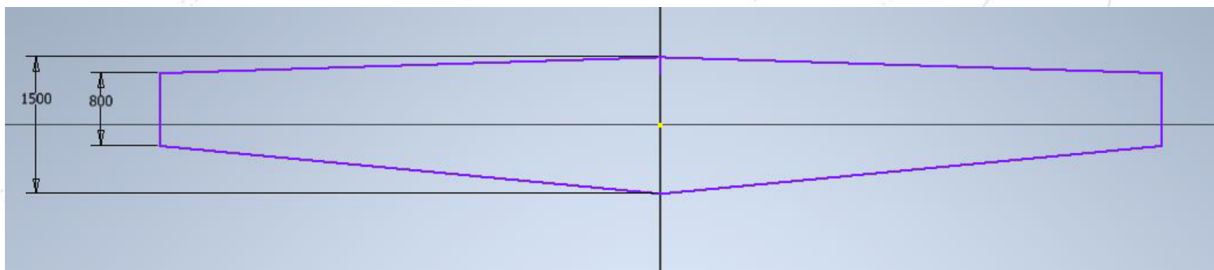


Figure 3.4 Wing geometry (Autodesk Inventor).

The C_{mac} (Mean Aerodynamic Chord) calculation for this wing geometry will also be required and will be computed graphically.

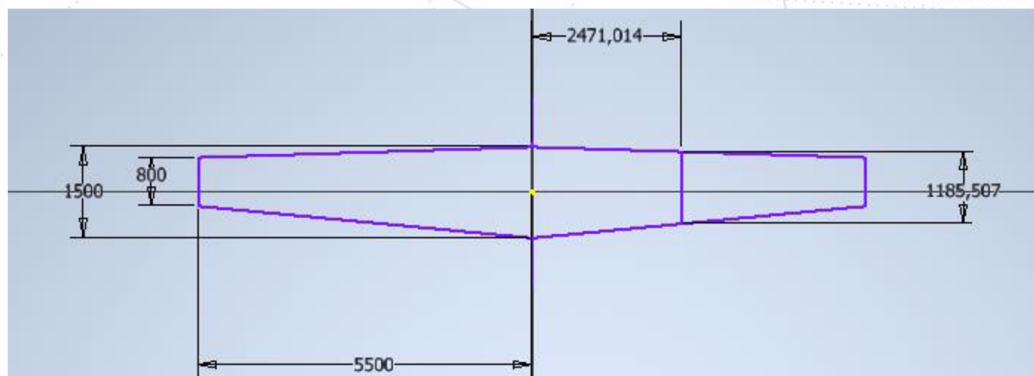


Figure 3.5 C_{mac} graphical computation (Autodesk Inventor).

3.1.3 Wing shape verification

Now it is necessary to check whether we can achieve the needed lift with the selected airfoil and wing shape. This will be checked using Glauert III software:

	L [m]	c [m]	clp [1]	clalfa [1]	alfa0 [°]
Wing root	0	1,5	1,74	6,1879	-5,5
Wing tip	5,5	0,8	1,74	6,1879	-5,5

Figure 3.6 Simulation inputs 1 (Glauert III).

Results overview:

Area of the wing $S = 12,65 \text{ m}^2$
 Aspect ratio $\Lambda = 9,565$
 Max. lift coefficient of the wing is $C_{lwingmax} = 1,648$
 Lift curve slope of the wing = $5,0621 \text{ rad}^{-1}$
 Angle of zero-lift coefficient (in the wing root) $\text{Alfa0wing} = -5,5^\circ$ (without the influence of flaps and ailerons)
 Glauert coefficient $\delta = 0,0246$ (for the calculation of induced drag - calculated from normal distribution)
 Induced drag coefficient $C_{xi} = 0,0926$ (for the lift coefficient of the wing $C_{lwing} = 1,648$)

theta	z	c	cln	cl0	claisym	claiantis	clfl	clidam	clp	cltotal
0	5,5	0,8	0	0	0	0	0	0	1,74	0
4,737	5,481	0,802	0,2422	0	0	0	0	0	1,74	0,3991
9,474	5,425	0,81	0,4519	0	0	0	0	0	1,74	0,7448
14,211	5,332	0,821	0,6199	0	0	0	0	0	1,74	1,0217
18,947	5,202	0,838	0,7488	0	0	0	0	0	1,74	1,2341
23,684	5,037	0,859	0,8449	0	0	0	0	0	1,74	1,3924
28,421	4,837	0,884	0,9151	0	0	0	0	0	1,74	1,5081
33,158	4,604	0,914	0,9652	0	0	0	0	0	1,74	1,5907
37,895	4,34	0,948	1,0006	0	0	0	0	0	1,74	1,6489
42,632	4,046	0,985	1,0249	0	0	0	0	0	1,74	1,689
47,368	3,725	1,026	1,0409	0	0	0	0	0	1,74	1,7154
52,105	3,378	1,07	1,0505	0	0	0	0	0	1,74	1,7312
56,842	3,008	1,117	1,0551	0	0	0	0	0	1,74	1,7388
61,579	2,618	1,167	1,0555	0	0	0	0	0	1,74	1,7395
66,316	2,209	1,219	1,0524	0	0	0	0	0	1,74	1,7343
71,053	1,786	1,273	1,0459	0	0	0	0	0	1,74	1,7236
75,789	1,35	1,328	1,0359	0	0	0	0	0	1,74	1,7072
80,526	0,905	1,385	1,022	0	0	0	0	0	1,74	1,6843
85,263	0,454	1,442	1,0029	0	0	0	0	0	1,74	1,6528
90	0	1,5	0,975	0	0	0	0	0	1,74	1,6068

theta - angle defining the position of the section (see help)
 z - position of the section on the half of wingspan (0 = wing root)
 c - Airfoil chord length
 cln - value of the lift coefficient of normal distribution
 cl0 - value of the lift coefficient of zero distribution
 claisym - value of the lift coefficient of aileron symmetric distribution (zero)
 claiantisym - value of the lift coefficient of aileron antisymmetric distribution
 clfl - value of the lift coefficient of flap distribution (zero)
 clidam - value of local lift coefficient of aerodynamic damping
 clp - value of airfoil lift coefficient
 cltotal - value of total lift coefficient

Figure 3.7 Simulation results (Glauert III).

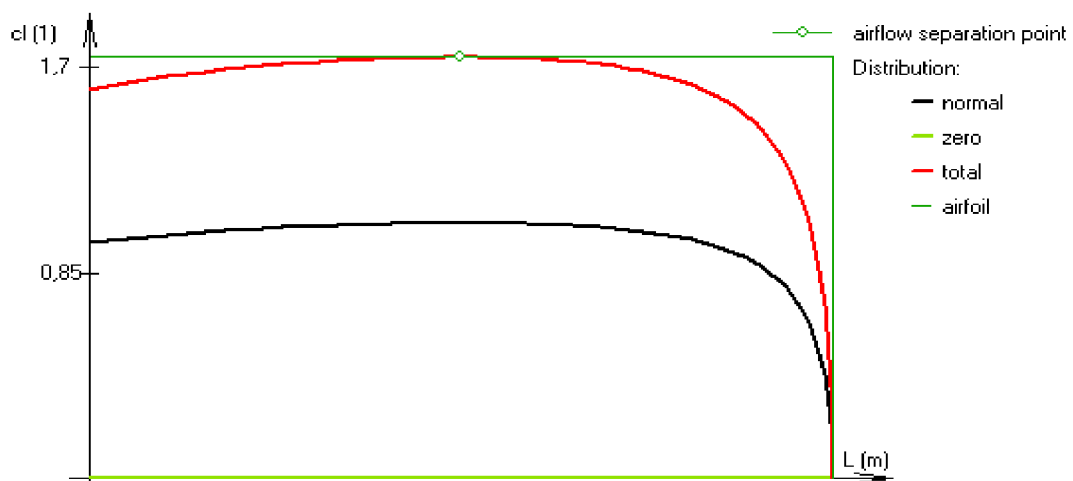


Figure 3.8 Lift distribution along wingspan (Glauert III).

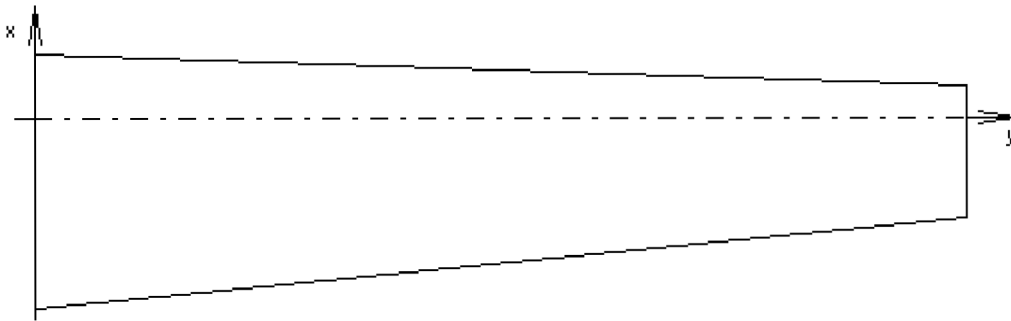


Figure 3.9 Glauert's wing planform detail.

This can be computed graphically using the next chart or mathematically by the Lift formula.

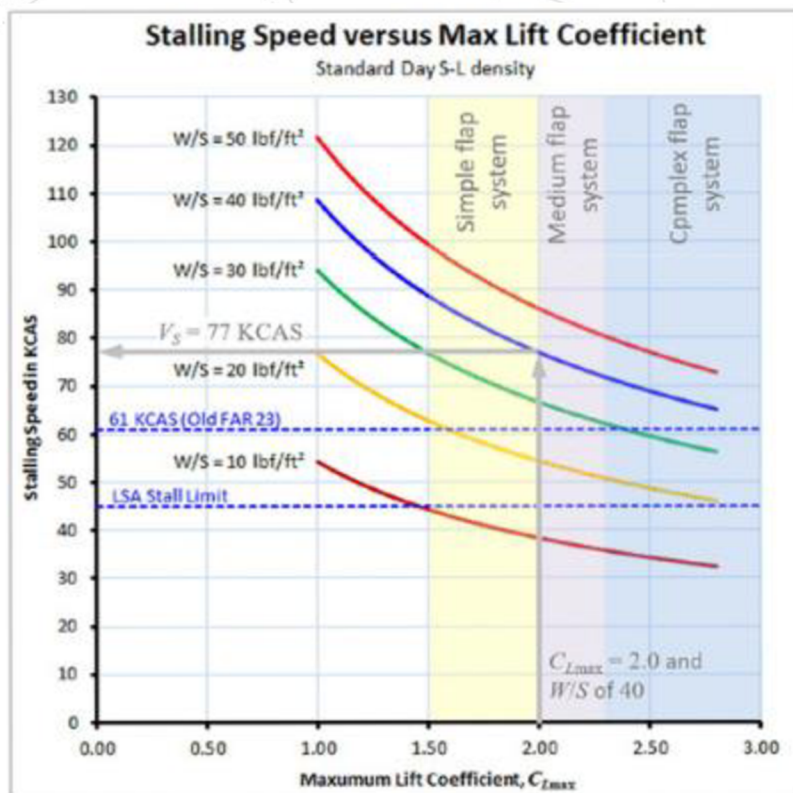


Figure 3.10 Stalling speed vs Clmax [6].

By the use of the maximum lift coefficient value of the aircraft (90% of the wing coefficient), we can determine the minimum speed of the aircraft and verify its compliance with the CS 23 requirements [7].

$$V_{min} = \sqrt{\frac{2M_{tow} * g}{\rho * Cl(max) * A}} = 51,16 \text{ knots} < 61 \text{ knots}$$

As a result, the stall speed requirement has been confirmed, and based on these results, it can be concluded that the installation of flaps is not necessary in terms of the stall requirement.

3.2 Tail unit design

For the calculation of tail unit surfaces Raymer’s method for initial sizing is used:

$$S_{VT} = c_{VT} \bar{c}_w S_w / L_{VT}$$

$$S_{HT} = c_{HT} \bar{c}_w S_w / L_{HT}$$

Figure 3.11 Expressions for vertical and horizontal surfaces [6].

	Typical values	
	Horizontal c_{HT}	Vertical c_{VT}
Sailplane	0.50	0.02
Homebuilt	0.50	0.04
General aviation—single engine	0.70	0.04
General aviation—twin engine	0.80	0.07
Agricultural	0.50	0.04
Twin turboprop	0.90	0.08
Flying boat	0.70	0.06
Jet trainer	0.70	0.06
Jet fighter	0.40	0.07
Military cargo/bomber	1.00	0.08
Jet transport	1.00	0.09

Figure 3.12 Typical calculation values [6].

The arm size is given by the 60% of the fuselage’s length (4,2m)

With the coefficients from the table:

$$S_{HT} = 2.4994 \text{ m}^2$$

$$V_{HT} = 0.148 \text{ m}^2$$

These results are considered for the development of the 3D model design.

4. Propulsion unit

This chapter will focus on the selection of various components of the propulsion unit: the propeller, the electric motor, and the concept's battery system. The electric management system will not be discussed.

4.1 Engine selection

The basis for the engine selection has been choosing the manufacturer which offers the best power-to-weight-ratio. Once found it, a power margin is stabilized in the same way as the wing area, a comparison among various similar models. The manufacturer which offers the best power to weight ratio is Emrax, from it, 3 models have been compared.

4.1.1 Emrax 208

This particular engine model, despite being the smallest and least powerful

Mechanical		Electrical	
Type:	Axial flux motor / generator	Maximal battery voltage:	580 (HV) / 390 (MV) / 140 Vdc (LV)
Casing diameter:	208 mm	Peak power (at 6000 RPM):	86 kW
Axial length:	85 mm	Continuous power*:	up to 56 kW
Dry mass:	9,4 kg (AC) / 10,0 kg (CC) / 10,3 kg (LC)	Peak torque:	150 Nm
Stator cooling:	air (IP21) / combined (IP21) / liquid (IP65)	Continuous torque*:	up to 90 Nm
Mounting:	Front: 6x M8 threaded holes Back: 16x M8 threaded holes	Efficiency:	92-98%
Stacking:	Two motors can be stacked together to achieve doubled power / torque. For more info click here .	*Subject to drive cycle, thermal conditions and controller capability.	

Figure 4.1 EMRAX 208 specs [11].

within its family, still possesses specific specifications that are worth considering. These specifications include:

The model has been rejected for further consideration due to its low continuous power output, which does not align with the performance requirements and objectives of the concept.

4.1.2 Emrax 268

The most powerful of the family, these are its technical specifications:

Mechanical		Electrical	
Type:	Axial flux motor / generator	Maximal battery voltage:	800 (HV) / 650 (MV) / 250 Vdc (LV)
Casing diameter:	268 mm	Peak power (at 4500 RPM):	210 kW
Axial length:	91 mm	Continuous power*:	up to 117 kW
Dry mass:	21,4 kg (AC) / 21,9 kg (CC) / 22,3 kg (LC)	Peak torque:	500 Nm
Stator cooling:	air (IP21) / combined (IP21) / liquid (IP65)	Continuous torque*:	up to 250 Nm
Mounting:	Front: 6x M8 threaded holes Back: 16x M8 threaded holes	Efficiency:	92-98%
Stacking:	Two motors can be stacked together to achieve doubled power / torque. For more info click here .	*Subject to drive cycle, thermal conditions and controller capability.	

Figure 4.2 EMRAX 268 specs [11].

This engine is much more capable compared to the 208 version. However, its maximum power exceeds by far the target specifications of the project, since we will not need such power, this engine has been discarded in detriment for a more accurate for our objective.

4.1.3 Emrax 228

The model in between the previous two in term of specifications is the Emrax 228, which offers the next specifications:

Mechanical		Electrical	
Type:	Axial flux motor / generator	Maximal battery voltage:	710 (HV) / 520 (MV) / 180 Vdc (LV)
Casing diameter:	228 mm	Peak power (at 6500 RPM):	124 kW
Axial length:	86 mm	Continuous power*:	up to 75 kW
Dry mass:	12,9 kg (AC) / 13,2 kg (CC) / 13,5 kg (LC)	Peak torque:	230 Nm
Stator cooling:	air (IP21) / combined (IP21) / liquid (IP65)	Continuous torque*:	up to 130 Nm
Mounting:	Front: 6x M8 threaded holes Back: 16x M8 threaded holes	Efficiency:	92-98%
Stacking:	Two motors can be stacked together to achieve doubled power / torque. For more info click here .	*Subject to drive cycle, thermal conditions and controller capability.	

Figure 4.3 EMRAX 228 specifications [11].

It has been determined that the installation of engine model 228 is the most suitable option among the three available choices. While it may not enable us to achieve the desired maximum speed, it closely aligns with our requirements, opting for the next more powerful engine would result in excessive force for our study, significantly compromising the range and endurance.

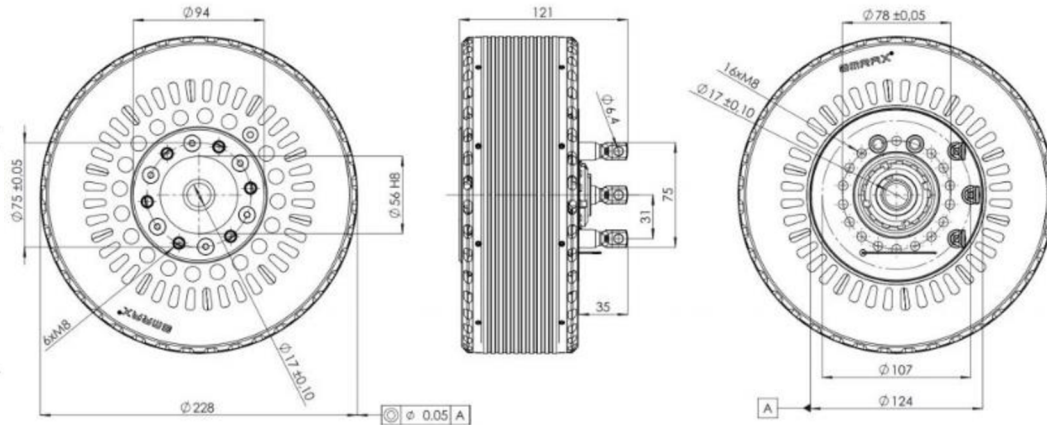


Figure 4.4 EMRAX 228 dimensions [11].

4.2 Propeller selection

One of the important characteristics will be the geometry of the propeller, including its dimensions and the number of blades, as it will greatly influence the efficiency of the propulsion unit.

Two-bladed propellers offer greater efficiency for low speeds and smaller aircraft due to their lower aerodynamic resistance compared to propellers with a higher number of blades. However, they may not generate as much thrust as three-bladed propellers. In this particular case, the requirement is not for a high-performance propeller, but rather an efficient one for low speeds. For this reason, it has been chosen a two-bladed metal propeller.

The size of the propeller will be determined by the expression.

$$D_p = 22 \sqrt[3]{P_{BHP}}$$

The result for this diameter is 185cm, this is quite close to the height of the aircraft, depending on the rigidity of the landing gear it would be needed to reduce the diameter and use a third blade. In this case it has been accepted as a safe value.

The propeller efficiency will be used in the performance chapter, it has been set an efficiency of 85%.

4.3 Battery selection

Regarding the battery, the selection criterion has been simple. The model with the highest energy density per kilogram and per volume in the current aeronautical market has been selected. Possible models used in automation has been discarded such as Tesla 8840 or Panasonic 2170.

The selected module for this aircraft is the **EPiC AV2300**, whose specifications are detailed in Table 17. A total of 41 modules will be installed to ensure extended operation of the aircraft. The use of this module will correspond mainly to its specifications, i.e. it will be counted the volume and weight needed for its specs.

A weight correction factor of 0.75 and a volume correction factor of 0.60 will be applied. These corrections accounts for the fact that in the arrays of modules, we will be utilizing the inner part of the AV2300 rather than the entire casing of each individual unit.

After applying these coefficients, the gravimetric energy density raises up to 280 wh/kg and the volumetric up to 383 wh/L. In comparison with the automotive industry examples named before:

		Tesla 4680	Panasonic 2170	ePIC AV 2300
Capacity	[wh]	86,62	18,56	2270
Volume	[L]	0,13	0,03	5,92
Weight	[kg]	0,355	0,068	8,104
Gravimetric energy density	[wh/kg]	244	272,94	280,11
Volumetric density	[wh/L]	650	535,86	383,55

Table 4.1 Batteries comparison [12].

Therefore, can be stated that with this battery we are working within realistic and safe approach to our project.



Figure 4.5 EPiC AV 2300 overview [13].

Nominal Capacity	Beginning of Life (BoL)	2.27	kWh
Temperature	Operating Charge ¹	10 to 45	°C
	Operating Discharge ¹	-20 to 60	°C
	Ground Survival	-55 to 85	°C
	Long-term Storage	-30 to 25	°C
Continuous Discharge Current ²	w/Passive Cooling	min of 2.5C or 300A	
	w/Active Cooling	min of 5.0C or 300A	
Peak Discharge Current	10 Second Pulse	min of 10.C or 600A	
Continuous Charge	w/Standard Charger	min of 1.0C or 150A	
	w/EPS DC Fast Charger	min of 3.0C or 300A	
Other	Estimated Cycle Life ³	2,000	Cycles
	Mass	11.35	kg
	Specific Energy	200	Wh/kg
	Dimensions	10.623" x 5.429" x 10.439"	
	Case Material	Aluminum	
	Cell Technology	Lithium-Ion	
	Thermal Management	Air (Passive) or Liquid (Active)	

Figure 4.6 Battery module specifications [13].

The energy storage system of the aircraft will be divided into two packs. The front one will consist of 21 single modules (, while the rear array will have 20 modules, resulting in a total of 41 modules and a combined energy capacity of 93.07 kWh. It should be noted that in order to prolong the battery's lifespan, manufacturers recommend utilizing it within the range of 20% to 80% capacity. For the purpose of this study, we will consider the range from 20% to 100%, reserving the remaining 20% for emergency situations. This equates to a usable energy capacity of 74.4 kWh.

4.3.1 Charging time calculation

The calculations in this chapter have been made based on the energy prices in Spain as of February 20, 2023. It's important to note that electricity prices in the current market are highly variable, so it is necessary to consider that they may differ from the current values.

Furthermore, it should be noted that the charging efficiency will not be 100%. This efficiency depends on various factors such as the quality of the installation, the battery itself, and environmental conditions like temperature. A charging efficiency factor of 0.85 has been applied, indicating that an additional 15% of energy will be required to charge the battery.

Additionally, electric vehicle charging points have been considered as potential locations to charge our aircraft. However, it is important to clarify that this scenario is not feasible. These charging points have been taken into account solely for the purpose of comparing different charging speeds and evaluating the charging time and cost under various situations.

For a full charge of the battery:

Place	Power [kW]	Price kWh [€]	Total price [€]	Total price [usd]	Time [min]
House general socket (Wallbox)	3,7	0,25	27,64	29,30	1524,3
Wallbox	7,4	0,29	32,07	33,99	762,2
Wallbox	11	0,31	34,28	36,33	512,7
Wallbox	22	0,35	38,70	41,02	256,4
Endesa X Charging point	43	0,4	44,23	46,88	131,2
Endesa X Charging point	50	0,42	46,44	49,23	112,8
Iberdrola superfast charging point	120	0,45	49,76	52,75	47,0
Ionity charging point	150	0,79	87,36	92,60	37,6
Wenea super charging point	200	0,49	54,18	57,44	28,2

Table 4.2 Speed and price comparison for full charge [14].

For the previously selected battery, the charging options are limited because the battery manufacturer does not recommend a charge higher than 50 kWh. Therefore, the two fastest possible charging options have been highlighted in bold.

For our case (20-100%):

Place	Power [kW]	Total price [eur]	Total price [usd]	Time [min]
House general socket (Wallbox)	3,7	22,12	23,44	1219,5
Wallbox	7,4	25,66	27,20	609,7
Wallbox	11	27,43	29,07	410,2
Wallbox	22	30,97	32,82	205,1
Endesa X Charging point	43	35,39	37,51	104,9
Endesa X Charging point	50	37,16	39,39	90,2
Iberdrola superfast charging point	120	39,81	42,20	37,6
Ionity charging point	150	69,89	74,09	30,1
Wenea super charging point	200	43,35	45,95	22,6

Table 4.3 Speed and price comparison (20-100%).

5. Structural design

The objective of this chapter is to assess the feasibility of the project in terms of the space required for the batteries and systems present in the aircraft, as well as the study of potential collisions between elements. Therefore, the inclusion of the tail unit, and other control surfaces structures has been excluded.

This structural design is not based on empirical studies or mathematical analysis, but rather on a layout derived from other aircraft modes.

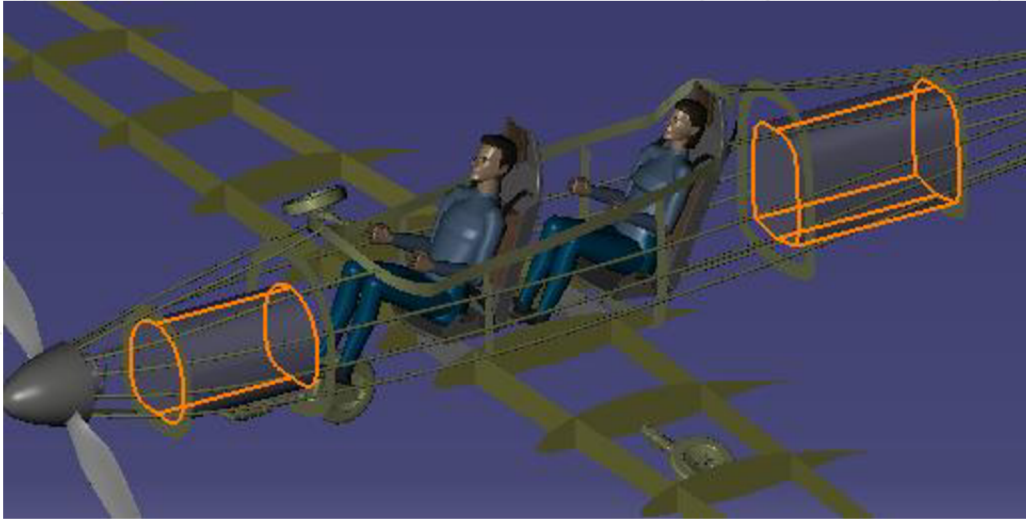


Figure 5.1 Aircraft structure overview (CATIA).

The most important aspect to verify in this chapter is the possibility of inclusion of the batteries, the spaces reserved for its inclusion are represented highlighted in the following picture .

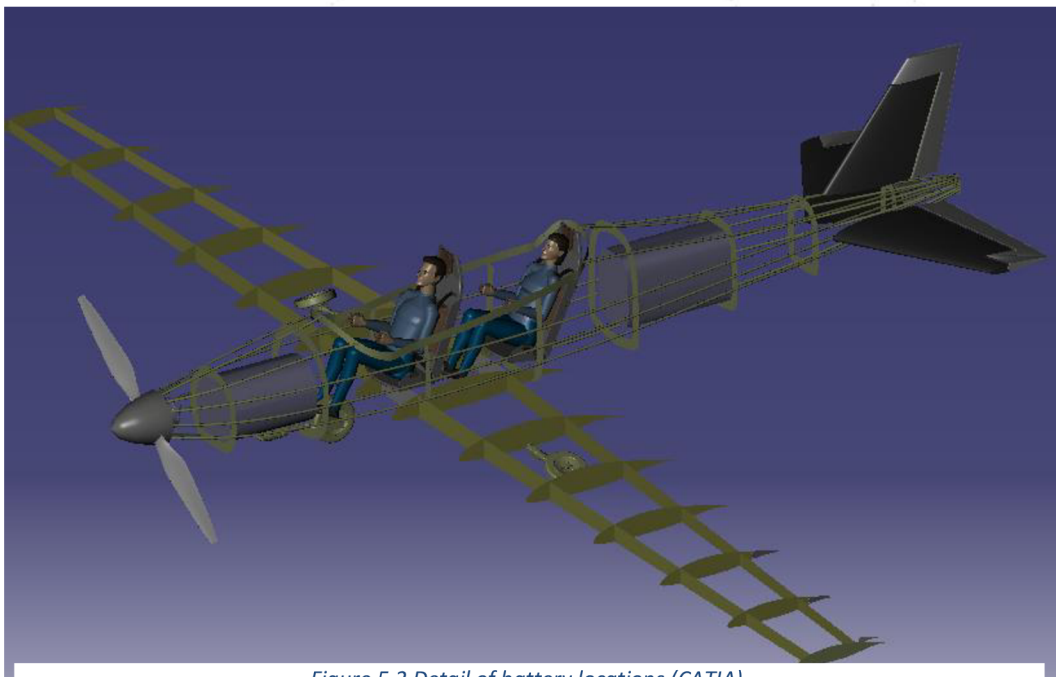


Figure 5.2 Detail of battery locations (CATIA).

With the specs from the table 4.1 we can estimate the needed volume para to carry that number of batteries.

Front battery volume required	[L]	118,37
Rear battery volume required	[L]	124,28

Table 5.1 Required battery volume.

And the available volume:



Figure 5.3 Front battery available volume (CATIA).

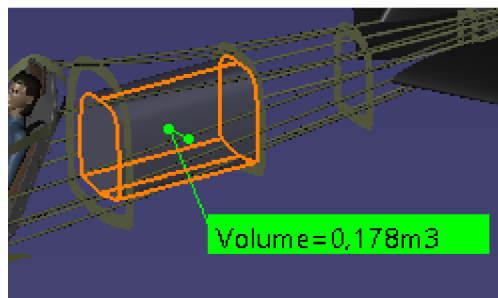


Figure 5.4 Rear battery available volume (CATIA).

The available volume exceeds the required, thus it is feasible the use of these batteries.

In addition to battery verification, the cabin space, landing gear, and collision between important design elements can be studied. These topics will be verified as follows:

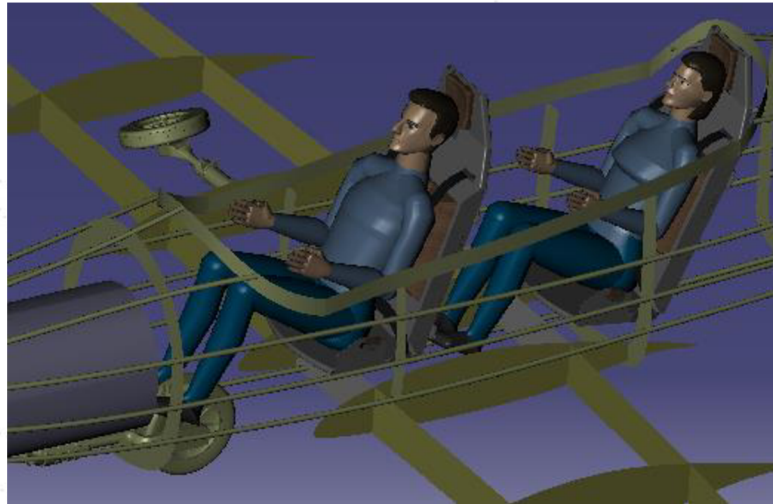


Figure 5.5 Available space in cabin (CATIA).

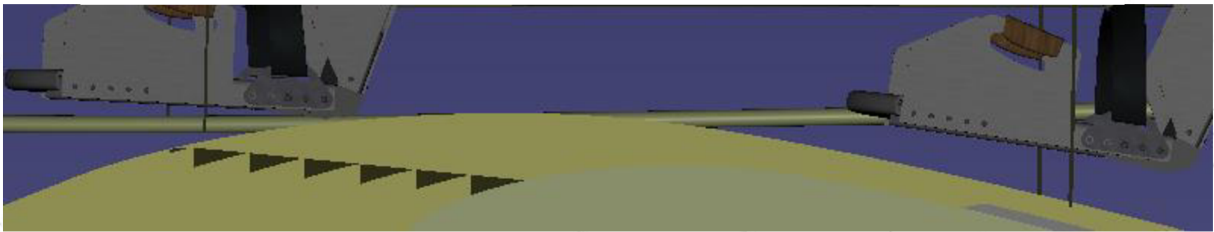


Figure 5.6 Verification of collision in seat's position (CATIA).

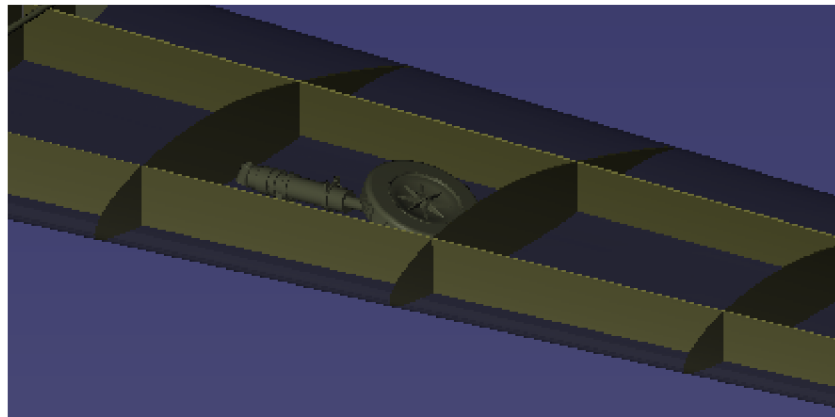


Figure 5.7 Main landing gear bay detail (CATIA).

The front landing gear would remain partially exposed, which would slightly impact the aerodynamic capabilities, although not significantly.

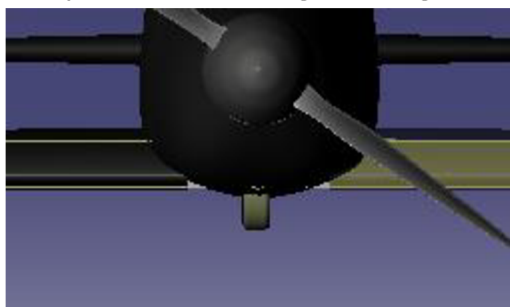


Figure 5.8 Partial exposure of the landing gear (CATIA).

6. Weight analysis

For this estimation we will be using Statistical Aircraft Component method [6] this consists in the calculation of them through expressions based on data taken from previous aircraft models. We can calculate the weight of a high number of components through this method, however some others will be calculated through other or simply taking their data from official specifications.

6.1 Component's weight estimation

Wing weight

$$W_W = 0.036 \cdot S_W^{0.758} W_{FW}^{0.0035} \left(\frac{AR_W}{\cos^2 \Lambda_{C/4}} \right)^{0.6} \times q^{0.006} \lambda^{0.04} \left(\frac{100 \cdot t/c}{\cos \Lambda_{C/4}} \right)^{-0.3} (n_z W_O)^{0.49}$$

Horizontal tail

$$W_{HT} = 0.016 (n_z W_O)^{0.414} q^{0.168} S_{HT}^{0.896} \left(\frac{100 \cdot t/c}{\cos \Lambda_{HT}} \right)^{-0.12} \cdot \left(\frac{AR_{HT}}{\cos^2 \Lambda_{HT}} \right)^{0.043} \lambda_{HT}^{-0.02}$$

Vertical tail

$$W_{VT} = 0.073 (1 + 0.2 F_{tail}) (n_z W_O)^{0.376} q^{0.122} S_{VT}^{0.873} \left(\frac{100 \cdot t/c}{\cos \Lambda_{VT}} \right)^{-0.49} \cdot \left(\frac{AR_{VT}}{\cos^2 \Lambda_{VT}} \right)^{0.357} \lambda_{VT}^{0.039}$$

Fuselage weight

$$W_{FUS} = 0.052 \cdot S_{FUS}^{1.086} (n_z W_O)^{0.177} I_{HT}^{-0.051} \left(\frac{I_{FS}}{d_{FS}} \right)^{-0.072} q^{0.241} + 11.9 (V_P \Delta P)^{0.271}$$

Main Landing Gear

$$W_{MLG} = 0.095 (n_l W_l)^{0.768} (L_m/12)^{0.409}$$

Nose Landing Gear

$$W_{NLG} = 0.125 (n_l W_l)^{0.566} (L_n/12)^{0.845}$$

Installed Engine Weight

Parameter obtained from the datasheet of the chosen engine:

$$W_{ENG} = 20,3 \text{ Kg}$$

Flight Control-system Weight

$$W_{CTRL} = 0.053I_{FS}^{1.536}b^{0.371}(n_z W_O \times 10^{-4})^{0.80}$$

Hydraulic System Weight

$$W_{HYD} = 0.001W_O$$

Avionics Systems Weight

$$W_{AV} = 2.117W_{LAV}^{0.933}$$

Electrical System Weight

$$W_{EL} = 12.57(W_{FS} + W_{AV})^{0.51}$$

Furnishings Weight

$$W_{FURN} = 0.0582W_O - 65$$

Passengers Weight

For this computation, we will use two configurations: light (1 passenger weighing 55kg) and heavy (2 passengers weighing 110kg each). To be on the safe side, the calculations for the model will be performed using the heavy setup.

Results of weight estimation in the light approach:

Element	Weight 1st calc [kg]
Pilot	55,0
Passenger	0,0
Wing	142,100
HTU	13,770
VTU	1,217
Fuselage	62,659
Main landing gear	57,421
Nose landing gear	9,072
Cowling	14,623
Engine	20,5
Flight. Control system	16,515

Hydraulic System	1,0
Avionics	2,584
Electrical system	36,180
Electrical Controller	8,1
Propeller	13,0
Furnishing	22,896
Front battery pack	169,229
Rear battery pack	163,440
TOTAL [kg]	809,305

Table 6.1 Weight estimation for light configuration.

As observed, the weight computation results in a value that is lower than the chosen target Maximum Take-off Weight (MTOW), indicating that there are still 91,376 usable kilograms available. This implies that there is a significant margin within the weight capacity of the aircraft to accommodate additional payload, equipment, or batteries while staying within the target MTOW limits, iteration for this setup won't be required due to this first calculation being the most restrictive.

Now for the heavy configuration:

Element	Weight 1st calc [kg]
Pilot	110,0
Passenger	110,0
Wing	142,100
HTU	13,770
VTU	1,217
Fuselage	62,659
Main landing gear	57,421
Nose landing gear	9,072
Cowling	14,623
Engine	20,5
Flight. Control system	16,515
Hydraulic System	1,0
Avionics	2,584
Electrical system	36,180
Electrical Controller	8,1
Propeller	13,0
Furnishing	22,896
Front battery pack	169,229
Rear battery pack	163,440
TOTAL [kg]	974,305

Table 6.2 Weight estimation for heavy configuration.

In this case, the computed result exceeds the initial estimated MTOW. To obtain more precise results, iterative calculations will be performed.

The estimation can be concluded after the third iteration. This final MTOW differs from the target by 10%. It's important to note that this change in MTOW will impact the stall capabilities of the aircraft. As a result, a thorough re-check and evaluation of the stall characteristics must be conducted.

Element	Weight 1st calc [kg]	First iteration	Second iteration	Third iteration
Pilot	110,0	110,0	110,0	110,0
Passenger	110,0	110,0	110,0	110,0
Wing	142,100	146,647	147,844	148,163
HTU	13,770	14,774	15,045	15,117
VTU	1,217	1,273	1,287	1,291
Fuselage	62,659	66,195	67,139	67,392
Main landing gear	57,421	60,231	60,990	61,193
Nose landing gear	9,072	9,072	9,072	9,072
Cowling	14,623	14,623	14,623	14,623
Engine	20,5	20,5	20,5	20,5
Flight. Control system	16,515	17,412	17,652	17,716
Hydraulic System	1,0	1,0	1,0	1,0
Avionics	2,584	2,584	2,584	2,584
Electrical system	36,180	39,167	39,978	40,195
Electrical Controller	8,1	8,1	8,1	8,1
Propeller	13,0	13,0	13,0	13,0
Furnishing	22,896	27,221	28,395	28,709
Front battery pack	169,229	169,229	169,229	169,229
Rear battery pack	163,440	163,440	163,440	163,440
TOTAL [kg]	974,305	994,467	999,877	1001,325

Table 6.3 Weight estimation iterations.

The estimation can be concluded after the third iteration. This final MTOW differs from the target by 10%. It's important to note that this change in MTOW will impact the stall capabilities of the aircraft. As a result, a thorough re-check and evaluation of the stall characteristics must be conducted.

$$V_{min} = \sqrt{\frac{2M_{tow} * g}{\rho * Cl(max) * A}} = 53,94 \text{ knots} < 61 \text{ knots}$$

It is still valid.

6.2 Gravity center estimation

To compute the center of gravity of the whole aircraft, each component has to be studied separately and as mentioned earlier, different scenarios involving varying weights for the pilot and passenger will be analyzed. Overall, it is crucial to ensure that the center of gravity falls within **18% to 35% of the Mean Aerodynamic Chord (MAC)** position. This range ensures that the design is on the right track.

To obtain the complete calculation of the gravity center, the following formula proposed by [6] will be employed:

$$X_{CG} = \frac{M_x}{W_{tot}} = \frac{1}{W_{tot}} \sum_{i=1}^N W_i \times x_i$$

The results are:

Element	Weight 1st calc [kg]	Xcg (m)	W*XcG (kg*m)
Pilot	55,0	2,2	121,0
Passenger	0,0	3,1	0,0
Wing	142,100	2,300	326,831
HTU	13,770	6,650	91,570
VTU	1,217	6,750	8,212
Fuselage	62,659	2,400	150,381
Main landing gear	57,421	3,000	172,263
Nose landing gear	9,072	1,500	13,608
Cowling	14,623	0,500	7,311
Engine	20,5	0,5	10,250
Flight. Control system	16,515	2,300	37,984
Hydraulic System	1,0	0,5	0,5
Avionics	2,584	2,000	5,169
Electrical system	36,180	2,000	72,360
Electrical Controller	8,1	1,1	8,9
Propeller	13,0	0,3	3,900
Furnishing	22,896	2,000	45,793
Front battery pack	169,229	1,250	211,536
Rear battery pack	163,440	4,300	702,792
TOTAL [kg]	809,305	1784,214	1990,368

Table 6.4 Gravity center position calculation for light setup.

% XCG/CMAC	XCG
35,37	2,52

The same applies for the other

Table 6.5 Gravity center position and verification.

the final iteration of configuration.

Element	Third iteration	Xcg (m)	W*XcG (kg*m)
Pilot	110,0	2,2	242,0
Passenger	110,0	3,1	341,0
Wing	148,163	2,300	340,775
HTU	15,117	6,650	100,529
VTU	1,291	6,750	8,717
Fuselage	67,392	2,400	161,741
Main landing gear	61,193	3,000	183,580
Nose landing gear	9,072	1,500	13,608
Cowling	14,623	0,500	7,311
Engine	20,5	0,5	10,250
Flight. Control system	17,716	2,300	40,746
Hydraulic System	1,0	0,5	0,5
Avionics	2,584	2,000	5,169
Electrical system	40,195	2,000	80,390
Electrical Controller	8,1	1,1	8,9
Propeller	13,0	0,3	3,900
Furnishing	28,709	2,000	57,419
Front battery pack	169,229	1,250	211,536
Rear battery pack	163,440	4,300	702,792
TOTAL [kg]	1001,325	2147,977	2520,873

Table 6.6 Gravity center position calculation for heavy setup.

% XCG/CMAC	XCG
30,44	2,46

Table 6.7 Gravity center position and verification

In the light setup, we are within the acceptable margin, but not in the heavy configuration. However, considering that these are extreme cases and the deviation is only 0.37%, it can be concluded that this is not a significant concern, and we would be within the margin in almost all cases.

7. Aircraft performance analysis

In this chapter, calculations will be performed to determine the theoretical performance specifications for the designed aircraft. The focus will be on key aspects of electric aircraft and the specifications that typically play a crucial role in the sale of aircrafts.

The following parameters will be computed:

- Drag polar.
- Power required and power available.
- Maximum speed.
- Rate of climb.
- Ceiling.
- Range.
- Endurance.
- Take-off distance.

Once these parameters have been calculated, a comparison can be made between the final computed specifications and the target specifications. This evaluation will help determine which goals have been successfully achieved.

It is important to note that the calculations have been performed for a specific range of speeds and altitudes relevant to the aircraft's intended operation.

7.1 Drag estimation

This estimation needs to be computed prior to the other performance parameters.

The guidelines for this chapter have been found at ***Airplane Design: Part VI*** [15].

The aircraft will be divided into separate parts: The Wing, body, and empennage. Each part will undergo individual analysis to compute the zero-lift drag coefficient (C_{D0}) and the induced drag (C_{Di}). These calculations provide valuable information about the aerodynamic efficiency and drag characteristics of the aircraft.

7.1.1 Wing drag estimation

The zero-lift drag coefficient has been estimated by the integration of the drag coefficient along the wingspan.

And the induced drag through the expression that relates it to the lift coefficient (Benson, s.f.) [16]

$$C_{Di} = \frac{Cl^2}{\pi \cdot AR \cdot e}$$

In the expression relating induced drag to the lift coefficient, the span efficiency factor (e) is introduced. This factor accounts for how effective the wing for minimizing induced drag. The value of e is assumed to be 0.9, representing a relatively efficient wing.

Computation results:

Wing drag coefficient				
Aoa (rad)	AoA (deg)	Cdlw	Cdow	Total Cdw
-0,1745	-10	0,0058	0,007	0,0128
-0,1571	-9	0,0035	0,007	0,0105
-0,1396	-8	0,0018	0,007	0,0088
-0,1222	-7	0,0006	0,007	0,0076
-0,1047	-6	0,0001	0,007	0,0071
-0,0960	-5,5	0,0000	0,007	0,0070
-0,0873	-5	0,0001	0,007	0,0071
-0,0698	-4	0,0006	0,007	0,0076
-0,0524	-3	0,0018	0,007	0,0088
-0,0349	-2	0,0035	0,007	0,0105
-0,0175	-1	0,0058	0,007	0,0128
0,0000	0	0,0087	0,007	0,0157
0,0175	1	0,0122	0,007	0,0192
0,0349	2	0,0162	0,007	0,0232
0,0524	3	0,0209	0,007	0,0279
0,0698	4	0,0260	0,007	0,0330
0,0873	5	0,0318	0,007	0,0388
0,1047	6	0,0382	0,007	0,0452
0,1222	7	0,0451	0,007	0,0521
0,1396	8	0,0526	0,007	0,0596
0,1571	9	0,0607	0,007	0,0677
0,1745	10	0,0693	0,007	0,0763
0,1920	11	0,0786	0,007	0,0856
0,2094	12	0,0884	0,007	0,0954
0,2269	13	0,0988	0,007	0,1058
0,2356	13,5	0,1004	0,007	0,1074

Table 7.1 Wing's drag computation results.

7.1.2 Body drag estimation

The estimation of body drag can be performed using the method outlined in [15]. In which, by considering the shape, surface area, and other relevant parameters of the aircraft's body, an estimation of the body drag is computed.

$$C_{D_{o_{fus}}} = R_{wf} C_{f_{fus}} \left(1 + 60 / (l_f / d_f) \right)^3 + 0.0025 (l_f / d_f) S_{wet_{fus}} / S + C_{D_{b_{fus}}}$$

Inputs			
Definition	Symbol	Units	Value
Wing/fus interference factor	Rwf	[-]	1,04
Turbulent flat plate skin friction coeff.	Cffus	[-]	0,0044
Fuselage length	Lf	[ft]	22,96
Aircraft max. Diameter	Df	[ft]	3,93
Wetted surface fuselage	Swetfus	[ft ²]	157,62

Table 7.2 Input values for body drag computation.

Body induced drag coefficient		
Aoa (rad)	AoA (deg)	Cdlb
-0,1745	-10	-0,0043
-0,1571	-9	-0,0031
-0,1396	-8	-0,0022
-0,1222	-7	-0,0015
-0,1047	-6	-0,0009
-0,0960	-5,5	-0,0007
-0,0873	-5	-0,0005
-0,0698	-4	-0,0003
-0,0524	-3	-0,0001
-0,0349	-2	0,0000
-0,0175	-1	0,0000
0,0000	0	0,0000
0,0175	1	0,0000
0,0349	2	0,0000
0,0524	3	0,0001
0,0698	4	0,0003
0,0873	5	0,0005
0,1047	6	0,0009
0,1222	7	0,0015
0,1396	8	0,0022
0,1571	9	0,0031
0,1745	10	0,0043
0,1920	11	0,0057
0,2094	12	0,0075
0,2269	13	0,0095
0,2356	13,5	0,0106

Table 7.3 Body's drag computation results.

7.1.3 Empennage drag estimation

Divided into different sections (HTU and VTU) as well. To compute the zero-lift drag coefficient, we will follow the procedure outlined [15], which is the basis for the following expression:

$$C_{D_{0w}} = (R_{wf}) (R_{LS}) (C_{f_w}) \{1 + L'(t/c) + 100(t/c)^4\} S_{wet_w} / S \tag{4.6}$$

Inputs			
Definition	Symbol	Units	Value
Wing/fuselage interference factor	Rwf	[-]	1
Turbulent flat plate skin friction coeff.	Rls	[-]	1,07
Fuselage length	Cfw	[-]	0,006
Max thickness location parameter	L'(airfoil)	[ft]	0,3281
Max thickness ratio	t/c	[-]	0,12
HTU Wetted area	Swet	[ft2]	22,0552
HTU Surface	S	[ft2]	11,0276

Table 7.4 HTU inputs.

Inputs			
Definition	Symbol	Units	Value
Wing/fus interference factor	Rwf	[-]	1
Turbulent flat plate skin friction coeff.	Rls	[-]	1,07
Fuselage length	Cfw	[-]	0,0058
Max thickness loc parameter	L'(airfoil)	[ft]	0,4921
Max thickness ratio	t/c	[-]	0,1200
HTU Wetted area	Swet	[ft2]	9,956615
VTU Surface	S	[ft2]	19,9132

Table 7.5 VTU inputs.

The inputs result in these coefficients:

Cdo HTU	0,001102
Cdo VTU	0,000245

Table 7.6 Zero lift drag coefficients for tail unit components.

The computation of the drag coefficient due to lift is a bit more complicated, it is needed to compute first the pitching moment of the wing and its lift due to the fact that in order to be stable, the tail unit needs to create lift on the other way of

the wings as is observed in the figure. Knowing the geometry of the aircraft and the lift generated by the wing will allow us to estimate the lift coefficient of the tail unit and then, its drag due to lift.

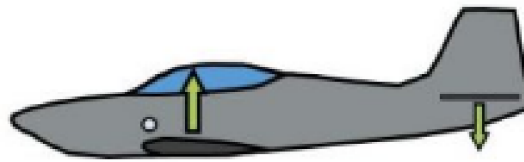


Figure 7.1 Lift forces generated by wings and HTU [17].

Wingspan distance (m)	Cl(y)	Cm(y)
0,000	1,3119	-0,14681
0,547	1,3337	-0,14397
1,087	1,3577	-0,14397
1,634	1,3721	-0,14225
2,181	1,3866	-0,14113
2,728	1,3866	-0,14113
3,245	1,3866	-0,14113
3,799	1,3721	-0,14225
4,354	1,3289	-0,14225
4,893	1,2280	-0,14507
5,290	1,0069	-0,14965
5,5	0,3246	-0,14225

Table 7.7 Lift and moment coefficient distribution.

The integration of the Cm along the wingspan will provide us with the total pitching moment coefficient of the wing. By simple torque computations we obtain the lift of the HTU.

$$Cd_i = \frac{Cl^2}{AR e \pi}$$

Where e refers to the efficiency factor and equals to 0,5,

Definition	Symbol	Units	Value
Wing pitching moment coefficient	Cm	[-]	0,124
Wing pitching moment	M	[N.m]	4833,14
Lift coefficient HTU	Cl	[-]	0,27
Lift HTU	L	[N]	1460,6

Table 7.8 Computed results for HTU I.

The total for the tail:

Tail drag coefficient.					
Aoa (rad)	AoA (deg)	Cl	Cdlt	Cdo	Cdtail
-0,1745	-10	0,2731	0,0156	0,0013	0,0169
-0,1571	-9	0,2731	0,0156	0,0013	0,0169
-0,1396	-8	0,2731	0,0156	0,0013	0,0169
-0,1222	-7	0,2731	0,0156	0,0013	0,0169
-0,1047	-6	0,2731	0,0156	0,0013	0,0169
-0,0960	-5,5	0,2731	0,0156	0,0013	0,0169
-0,0873	-5	0,2731	0,0156	0,0013	0,0169
-0,0698	-4	0,2731	0,0156	0,0013	0,0169
-0,0524	-3	0,2731	0,0156	0,0013	0,0169
-0,0349	-2	0,2731	0,0156	0,0013	0,0169
-0,0175	-1	0,2731	0,0156	0,0013	0,0169
0,0000	0	0,2731	0,0156	0,0013	0,0169
0,0175	1	0,2731	0,0156	0,0013	0,0169
0,0349	2	0,2731	0,0156	0,0013	0,0169
0,0524	3	0,2731	0,0156	0,0013	0,0169
0,0698	4	0,2731	0,0156	0,0013	0,0169
0,0873	5	0,2731	0,0156	0,0013	0,0169
0,1047	6	0,2731	0,0156	0,0013	0,0169
0,1222	7	0,2731	0,0156	0,0013	0,0169
0,1396	8	0,2731	0,0156	0,0013	0,0169
0,1571	9	0,2731	0,0156	0,0013	0,0169
0,1745	10	0,2731	0,0156	0,0013	0,0169
0,1920	11	0,2731	0,0156	0,0013	0,0169
0,2094	12	0,2731	0,0156	0,0013	0,0169
0,2269	13	0,2731	0,0156	0,0013	0,0169
0,2356	13,5	0,2731	0,0156	0,0013	0,0169

Table 7.9 Tail drag computation results.

7.1.4 Total drag

Once obtained all the previous results we can compute the total of the aircraft:

Total drag coefficient			
Aoa (rad)	AoA (deg)	Cl	Cd
-0,1745	-10	-0,3578	0,0410
-0,1571	-9	-0,2783	0,0376
-0,1396	-8	-0,1988	0,0349
-0,1222	-7	-0,1193	0,0330
-0,1047	-6	-0,0398	0,0319
-0,0960	-5,5	0,0000	0,0316
-0,0873	-5	0,0398	0,0315
-0,0698	-4	0,1193	0,0318
-0,0524	-3	0,1988	0,0328
-0,0349	-2	0,2783	0,0345
-0,0175	-1	0,3578	0,0367
0,0000	0	0,4373	0,0396
0,0175	1	0,5168	0,0431
0,0349	2	0,5964	0,0472
0,0524	3	0,6759	0,0519
0,0698	4	0,7554	0,0572
0,0873	5	0,8349	0,0632
0,1047	6	0,9144	0,0700
0,1222	7	0,9939	0,0775
0,1396	8	1,0735	0,0857
0,1571	9	1,1530	0,0947
0,1745	10	1,2325	0,1045
0,1920	11	1,3120	0,1152
0,2094	12	1,3915	0,1267
0,2269	13	1,4710	0,1391
0,2356	13,5	1,4832	0,1419

Table 7.10 Total drag coefficient results.

7.2 Drag polar

The drag polar of an aircraft is a graphical representation of the relationship between the aircraft's coefficient of lift (C_L) and coefficient of drag (C_D) at various flight conditions. It provides a summary of the aircraft's aerodynamic performance in terms of lift and drag. Its shape is given by the characteristics

of the concept, including the shape of the wing, the airfoil and the overall layout of the aircraft.

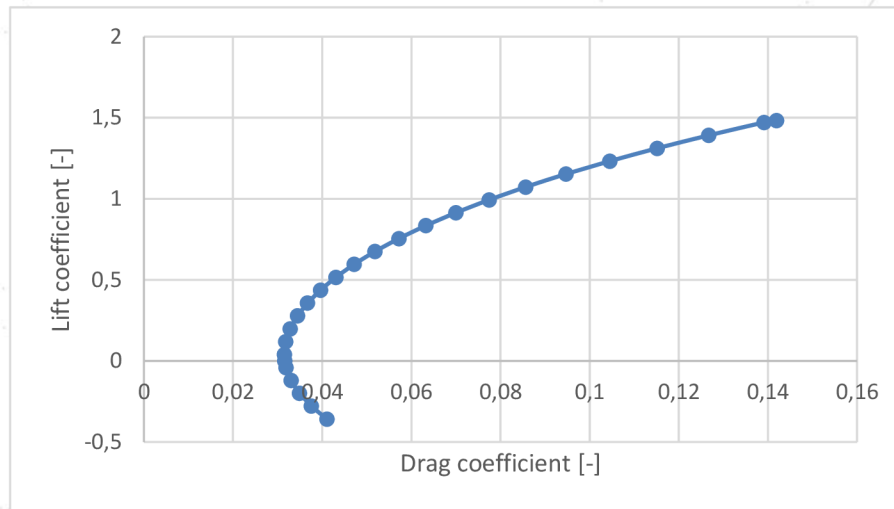


Figure 7.2 Aircraft drag polar.

7.3 Power required and available

The power available is the amount of power that the propeller or engine can generate. It represents the maximum power output that the propulsion system can provide to impulse the aircraft. On the other hand, power required refers to the amount of power needed to overcome the drag of the aircraft at a specific speed and altitude [18].

The relationship between these two parameters is critical when determining the aircraft's performance capabilities.

v[km/h]	Pavailable [KW]				
130	94,9904	94,9904	94,9904	94,9904	94,9904
140	97,1674	97,1674	97,1674	97,1674	97,1674
150	98,9969	98,9969	98,9969	98,9969	98,9969
160	100,5269	100,5269	100,5269	100,5269	100,5269
170	101,7985	101,7985	101,7985	101,7985	101,7985
180	102,8452	102,8452	102,8452	102,8452	102,8452
190	103,6935	103,6935	103,6935	103,6935	103,6935
200	104,3625	104,3625	104,3625	104,3625	104,3625
210	104,8643	104,8643	104,8643	104,8643	104,8643
220	105,2035	105,2035	105,2035	105,2035	105,2035
230	105,3776	105,3776	105,3776	105,3776	105,3776
240	105,3769	105,3769	105,3769	105,3769	105,3769
250	105,1844	105,1844	105,1844	105,1844	105,1844
260	104,7758	104,7758	104,7758	104,7758	104,7758
270	104,1198	104,1198	104,1198	104,1198	104,1198

280	103,1777	103,1777	103,1777	103,1777	103,1777
290	101,9034	101,9034	101,9034	101,9034	101,9034
Altitude [km]	0	2	3	4	4,5

Table 7.11 Power available results.

v[km/h]	Prequired [kW]				
130	35,4588	38,5986	40,8026	43,4996	45,0533
140	36,6204	38,8767	40,6295	42,8624	44,1773
150	38,4507	39,7943	41,0906	42,8608	43,9403
160	40,9385	41,3254	42,1518	43,4519	44,2948
170	44,0825	43,4560	43,7924	44,6080	45,2093
180	47,8890	46,1810	46,0014	46,3120	46,6635
190	52,3693	49,5020	48,7752	48,5550	48,6459
200	57,5388	53,4252	52,1155	51,3341	51,1511
210	63,4161	57,9607	56,0282	54,6508	54,1785
220	70,0220	63,1215	60,5224	58,5103	57,7313
230	77,3791	68,9226	65,6095	62,9206	61,8157
240	85,5118	75,3811	71,3031	67,8916	66,4401
250	94,4452	82,5154	77,6183	73,4354	71,6147
260	104,2058	90,3450	84,5713	79,5652	77,3513
270	114,8205	98,8903	92,1797	86,2953	83,6628
280	126,3171	108,1727	100,4616	93,6412	90,5633
290	138,7237	118,2139	109,4359	101,6190	98,0675
Altitude [km]	0	2	3	4	4,5

Table 7.12 Power required results.

In green: Achievable regimes within the maximum continuous power (<75kW).
 In yellow: Achievable regimes with temporal power output (75kW<<124kW).
 In red: Not achievable regimes (>124kW) or (P.required > P.available)

In graphical form:

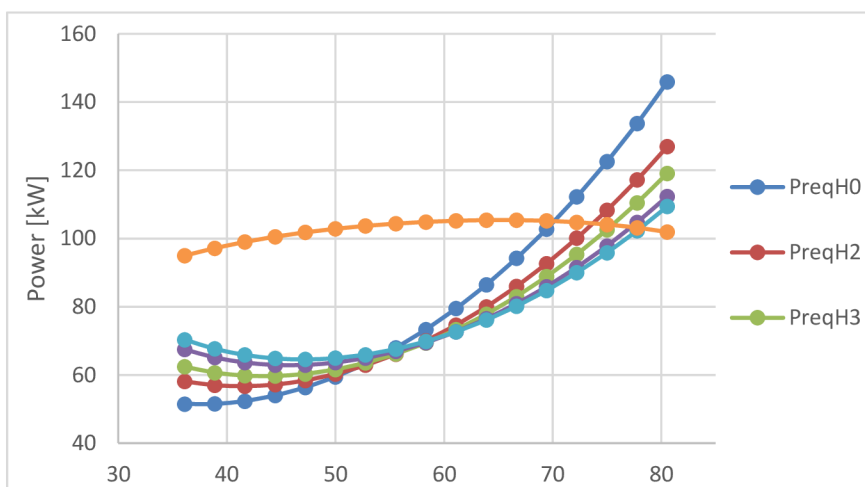


Figure 7.3 Power required and power available v velocity.

7.4 Maximum speed.

These values are obtained from the previous graph (7.3), they are determined by the point of intersection between the power required and power available curves.

H [km]	0	2	3	4	4,5
V max [Km/h]	252,11	266,4	271,8	279	280,28

Table 7.13 Maximum speed per altitude.

7.5 Rate of climb.

The rate of climb is defined as the velocity at which an aircraft is capable of gaining altitude. It is typically expressed in feet per minute or meters per second [18].

This value depends on different factors of the aircraft such as engine power, air density, and aerodynamic design. A higher rate of climb will allow the aircraft to quickly reach higher altitudes, while a shallower climbing angle requires more time to achieve greater heights.

As mentioned before, the power excess is an important factor when defining this topic due to the fact that the highest power excess will mean the highest rate of climb as we can see in the charts in bold value (150km/h and 0m).

v(km/h)	Pexcess [KW]				
130	43,5004	36,8787	32,5840	27,5124	24,6507
140	45,6609	40,1715	36,4772	32,0394	29,5099
150	46,6525	42,2913	39,1829	35,3548	33,1417
160	46,5632	43,3472	40,8220	37,5926	35,6869
170	45,4568	43,4208	41,4856	38,8541	37,2526
180	43,3781	42,5714	41,2411	39,2155	37,9193
190	40,3555	40,8405	40,1368	38,7323	37,7464
200	36,4035	38,2539	38,2046	37,4426	36,7753
210	31,5242	34,8241	35,4623	35,3698	35,0323
220	25,7086	30,5516	31,9152	32,5242	32,5302
230	18,9374	25,4259	27,5572	28,9041	29,2696
240	11,1816	19,4262	22,3717	24,4970	25,2400
250	2,4030	12,5222	16,3321	19,2802	20,4208
260	-7,4455	4,6744	9,4026	13,2215	14,7814
270	-18,4194	-4,1656	1,5383	6,2794	8,2821
280	-30,5825	-14,0546	-7,3142	-1,5963	0,8742
290	-44,0067	-25,0577	-17,2170	-10,4645	-7,4994
Altitude [km]	0	2	3	4	4,5

Table 7.14 Power excess results.

v(km/h)	Rate of climb [m/s]				
130	4,4340	3,7591	3,3213	2,8044	2,5127
140	4,6543	4,0947	3,7182	3,2658	3,0080
150	4,7553	4,3108	3,9939	3,6037	3,3782
160	4,7462	4,4184	4,1610	3,8318	3,6376
170	4,6335	4,4259	4,2287	3,9604	3,7972
180	4,4216	4,3393	4,2037	3,9973	3,8651
190	4,1135	4,1629	4,0912	3,9480	3,8475
200	3,7106	3,8992	3,8942	3,8166	3,7485
210	3,2133	3,5496	3,6147	3,6053	3,5709
220	2,6205	3,1142	3,2531	3,3152	3,3158
230	1,9303	2,5917	2,8089	2,9462	2,9835
240	1,1397	1,9801	2,2804	2,4970	2,5727
250	0,2449	1,2764	1,6647	1,9652	2,0815
260	-0,7589	0,4765	0,9584	1,3477	1,5067
270	-1,8775	-0,4246	0,1568	0,6401	0,8442
280	-3,1173	-1,4326	-0,7455	-0,1627	0,0891
290	-4,4856	-2,5542	-1,7549	-1,0667	-0,7644
Altitude [km]	0	2	3	4	4,5

Table 7.15 Rate of climb results.

Depicted graphically:

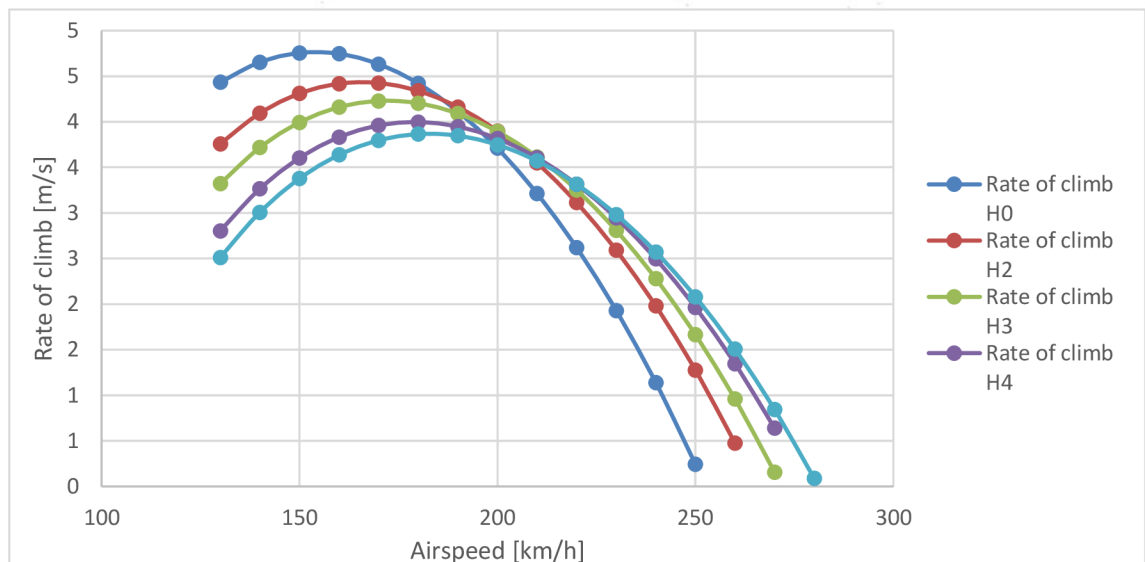


Figure 7.4 Rate of climb v velocity.

7.6 Operative ceiling

The service ceiling is defined as the maximum altitude an aircraft can reach while maintaining steady and level flight under standard atmospheric conditions. It means the highest operational altitude where the aircraft can function effectively and safely.

Several factors contribute to this value, including design, engine performance, weight, and environmental conditions. In the case of the electric model, the propulsive system is not a limiting factor for altitude, but the lack of pressurization in the aircraft will set the limit.

The human body is adapted to the conditions of life on Earth's surface. It relies on a consistent intake of oxygen into the lungs at a specific pressure to adequately saturate the hemoglobin found in red blood cells.

As altitude increases and atmospheric pressure decreases, there is a reduction in the partial pressure of oxygen. This decrease in oxygen availability can have effects on the human body. The symptoms that result from this condition are commonly known as Acute Mountain Sickness (AMS) or Altitude Sickness.

The symptoms of Acute Mountain Sickness (AMS) vary depending on the altitude of the aircraft:

-Up to 1,5km: Minor symptoms (hyperventilation - rapid and deep breathing, heartbeat increase)

-From 1,5 to 2km: First symptoms in brain nervous tissue (deterioration of three dimensional and scotopic vision)

-From 4 to 5km: Significant damage to the cerebral cortex function and parts of the central nervous system (breathing obstructions/shortness of breath, muscle weakness, nausea, etc.)

Generally talking, the safe limit for a human body is set to 1 hour of flight at the altitude of 3.5km. For long-haul flights it is 3km [19].

Having all these in mind, the operational ceiling has been set to **4500m**.

7.7 Range

The range is defined as the maximum distance covered by the aircraft under constant altitude and speed conditions without refueling or recharging. The peak range is commonly reached under circumstances where the lift-to-drag ratio is maximum.

For this computation, the analysis will focus on the maximum possible range, using the full capacity of the battery.

The calculations in this section are derived from the equation developed by Lochie Ferrier, as presented on the webpage [20].

$$R = E * \frac{M_{batt}}{M_{aircraft}} * \frac{1}{g} * \frac{L}{D} * N_{total}$$

In highlighted can be observed the maximum range for each studied altitude and it's relative lift-drag ratio.

v(km/h)	L/D				
130	6,8804	6,0964	5,6768	5,2502	5,0366
140	7,4073	6,6939	6,2864	5,8580	5,6390
150	7,8093	7,2087	6,8341	6,4230	6,2072
160	8,0800	7,6255	7,3030	6,9283	6,7246
170	8,2226	7,9359	7,6812	7,3601	7,1775
180	8,2487	8,1383	7,9626	7,7091	7,5552
190	8,1749	8,2380	8,1467	7,9706	7,8514
200	8,0200	8,2445	8,2383	8,1445	8,0641
210	7,8031	8,1708	8,2459	8,2349	8,1951
220	7,5418	8,0311	8,1805	8,2490	8,2497
230	7,2511	7,8396	8,0543	8,1961	8,2355
240	6,9434	7,6095	7,8795	8,0865	8,1615
250	6,6285	7,3524	7,6677	7,9308	8,0375
260	6,3138	7,0782	7,4291	7,7390	7,8732
270	6,0045	6,7949	7,1728	7,5203	7,6775
280	5,7046	6,5088	6,9059	7,2828	7,4586
290	5,4163	6,2247	6,6344	7,0331	7,2237
Altitude [km]	0	2	3	4	4,5

Table 7.16 Lift-drag ratio results.

v(km/h)	Range [km]				
130	179,8	159,7	148,7	137,5	131,9
140	198,5	179,3	168,4	157,0	151,1
150	213,2	196,8	186,6	175,4	169,5
160	224,0	211,4	202,5	192,1	186,4
170	230,9	222,8	215,6	206,6	201,5
180	233,9	230,8	225,8	218,7	214,3
190	233,7	235,6	233,0	227,9	224,6
200	230,8	237,3	237,1	234,4	232,1
210	225,6	236,2	238,4	238,1	237,0
220	218,8	233,0	237,3	239,3	239,4
230	210,7	227,8	234,0	238,1	239,3
240	201,7	221,1	229,0	235,0	237,2
250	192,3	213,3	222,5	230,0	233,2
260	182,4	204,5	214,7	223,6	227,5
270	172,4	195,1	205,9	215,9	220,5
280	162,3	185,2	196,5	207,2	212,3
290	152,2	174,9	186,4	197,6	203,0
Altitude [km]	0	2	3	4	4,5

Table 7.17 Range results.

Graphically:

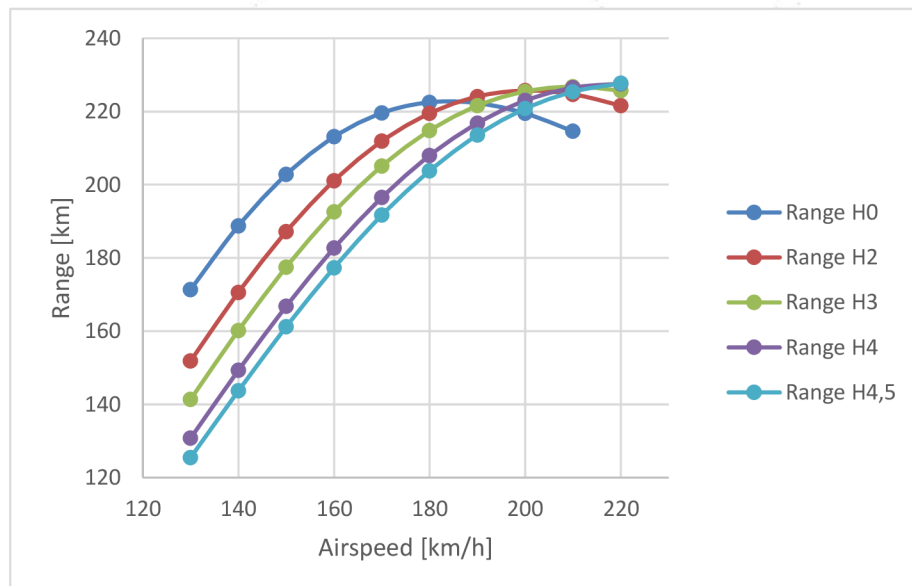


Figure 7.5 Range v velocity.

7.8 Endurance

Endurance is defined as the duration an aircraft can stay in the air with a fuel or battery charge. It differs from range in the unit of measurement, where endurance is expressed in terms of time, while range is measured in kilometres or miles.

In this project, endurance has been determined by the relationship between range and the corresponding speed [18].

v(km/h)	Endurance (0-100%) [min]				
130	82,98	73,70	68,61	63,47	60,89
140	85,06	76,86	72,18	67,27	64,74
150	85,28	78,72	74,64	70,14	67,79
160	84,01	79,28	75,93	72,03	69,90
170	81,48	78,62	76,10	72,91	71,13
180	77,97	76,92	75,27	72,89	71,42
190	73,80	74,40	73,57	71,97	70,91
200	69,23	71,18	71,12	70,33	69,64
210	64,46	67,49	68,12	68,03	67,70
220	59,67	63,54	64,71	65,26	65,28
230	54,96	59,43	61,05	62,12	62,42
240	50,44	55,27	57,24	58,74	59,29
250	46,15	51,19	53,39	55,20	55,96
260	42,09	47,19	49,54	51,60	52,50
270	38,31	43,36	45,77	47,99	48,99
280	34,78	39,69	42,10	44,40	45,48
290	31,49	36,19	38,56	40,89	42,00
Altitude [km]	0	2	3	4	4,5

Table 7.18 Endurance results.

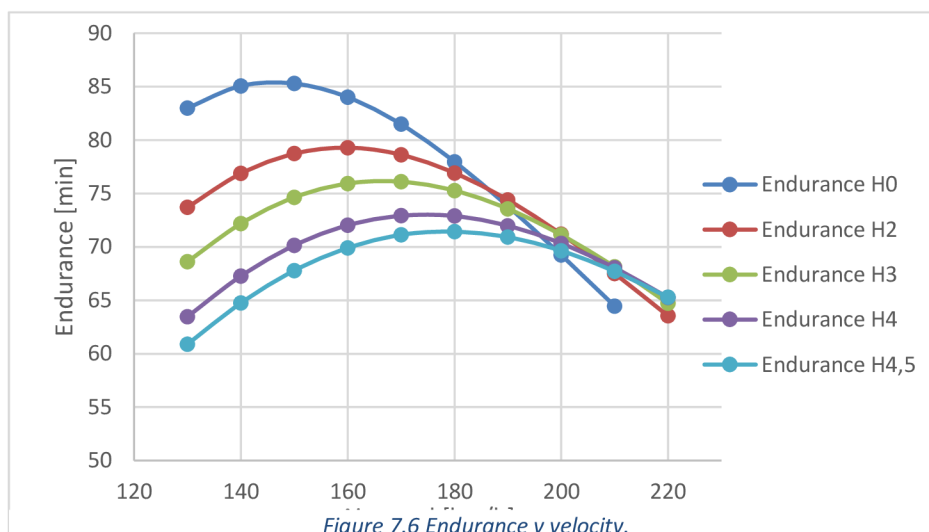


Figure 7.6 Endurance v velocity.

7.9 Take off distance

The takeoff distance is divided into two distinct segments: the ground run and the distance required for the aircraft to become airborne and reach a height of 15 meters or 50 feet. The total of these distances is considered the total take-off distance.

It is represented in the following figure.

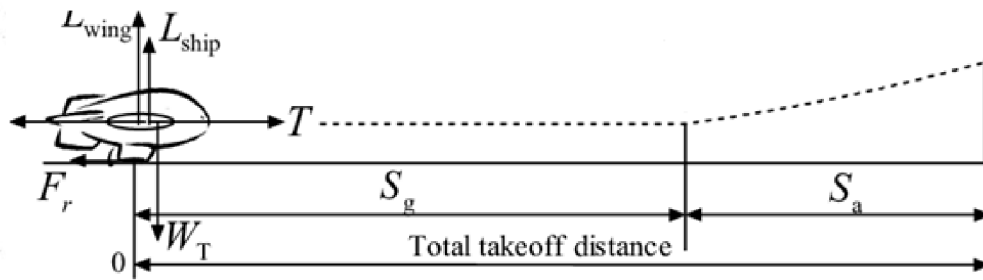


Figure 7.7 Schematic take-off representation [23].

The computed results:

$$S_a = 105,12 \text{ m}$$

$$S_g = 118,22 \text{ m}$$

$$S_{total} = 223,34 \text{ m}$$

Comparing to similar combustion engine models:

	take-off distance comparison		
Model	Cessna 172	Piper Cherokee	Elmio M1
Distance [m]	245,36	243,84	223,34
Variation [%]	109,86	109,18	100

Table 7.19 take-off comparison.

8. Aircraft cost analysis

The objective of this section is to determine the costs associated with the design and manufacturing of the aircraft. This analysis will allow us to evaluate the financial viability of the project and determine the necessary sales volume to ensure its profitability. Similar to the preceding chapter, our calculations will rely on the expressions outlined in the book [6].

8.1 Workhours calculation

Prior to the computation of the costs it is needed to estimate the workhours. A distinction in 3 categories will be made: engineering, tooling, and manufacturing. This differentiation is based on the different costs associated with the personnel performing these tasks.

Engineering Workhours (H_{ENGR}):

Referred to the hours needed for the design and perform of RDT+E.

$$H_{ENGR} = 0.0396 \cdot W_{airframe}^{0.791} \cdot V_H^{1.526} \cdot N^{0.183} \cdot F_{CERT_1} \cdot F_{CF_1} \cdot F_{COMP_1} \cdot F_{PRESS_1}$$

Tooling Workhours (H_{TOOL}):

Referred to the hours needed for the design and build of tools, molds, and other materials.

$$H_{TOOL} = 1.0032 \cdot W_{airframe}^{0.764} \cdot V_H^{0.899} \cdot N^{0.178} \cdot Q_m^{0.066} \cdot F_{CF_2} \cdot F_{COMP_2} \cdot F_{PRESS_2} \cdot F_{TAPER_2}$$

Manufacturing Labour Workhours (H_{MFG}):

Referred to the hours required to build the aircraft.

$$H_{MFG} = 9.6613 \cdot W_{airframe}^{0.74} \cdot V_H^{0.543} \cdot N^{0.524} \cdot F_{CERT_3} \cdot F_{CF_3} \cdot F_{COMP_3}$$

8.2 Costs calculation

Total Cost of Engineering (C_{ENGR}):

Using a rate of engineering labor in \$ per hour of 92\$/h (including taxes and other expenses). And a CPI rate of 1,2967 compared to the end of 2022 [24].

$$C_{ENGR} = H_{ENGR} \cdot R_{ENGR} \cdot CPI_{2012}$$

Total Cost of Development Support (C_{DEV}):

Overall costs of administration, logistics and other related activities required for the development of the project but that not necessarily have an influence on it.

$$C_{DEV} = 0.06458 \cdot W_{airframe}^{0.873} \cdot V_H^{1.89} \cdot N_P^{0.346} \cdot CPI_{2012} \cdot F_{CERT_5} \cdot F_{CF_5} \cdot F_{COMP_5} \cdot F_{PRESS_5}$$

Total Cost of Flight Test Operations (C_{FT}):

Related to aircraft certification and flight testing.

$$C_{FT} = 0.009646 \cdot W_{airframe}^{1.16} \cdot V_H^{1.3718} \cdot N_P^{1.281} \cdot CPI_{2012} \cdot F_{CERT_6}$$

Total Cost of Tooling (C_{TOOL}):

Costs of design, manufacture and maintaining the tools required for constructing the aircraft. Rate for tooling is of 61 \$/h [6].

$$C_{TOOL} = H_{TOOL} \cdot R_{TOOL} \cdot CPI_{2012}$$

Total Cost of Manufacturing (C_{MFG}):

The rate of manufacturing labor is 53 \$/h [6].

$$C_{MFG} = H_{MFG} \cdot R_{MFG} \cdot CPI_{2012}$$

Total Cost of Quality Control (C_{QC}):

$$C_{QC} = 0.13 \cdot C_{MFG} \cdot F_{CERT_9} \cdot F_{COMP_9}$$

Total Cost of Materials (C_{MAT}):

$$C_{MAT} = 24.896 \cdot W_{airframe}^{0.689} \cdot V_H^{0.624} \cdot N_P^{0.792} \cdot CPI_{2012} \cdot F_{CERT_{11}} \cdot F_{CF_{10}} \cdot F_{PRESS_{10}}$$

Fixed Cost (or Total Cost to Certify) (C_{fix}):

$$C_{fix} = C_{ENGR} + C_{DEV} + C_{FT} + C_{TOOL}$$

Variable Cost (C_{var}):

The variable cost comprises the cost of manufacturing labor, quality control, material and vendor supplied components (VSC), per unit.

$$C_{var} = \frac{C_{MFG} + C_{QC} + C_{MAT}}{N} + C_{VSC} + C_{INS}$$

The calculation of C_{VSC} depends on different parameters of the aircraft:

$$C_{VSC} = C_{VSC1} + C_{VSC2} + C_{VSC3} + C_{VSC4}$$

- **Fixed of retractable landing gear (C_{VSC1}):** In this case the aircraft has a retractable landing gear so following the book this parameter will be equal to 0.

- **Avionics (C_{VSC2}):** The avionics chosen for the aircraft are **Evolution 1500 Package** from Aspen Avionics, with a recommended retail price (installation included of) 17895\$ [25].

- **Engine cost (C_{VSC3}):** 3375,9 \$ (21% VAT) [11].

- **Propellers cost (C_{VSC4}):** We will be using a 72" two metal blade propellers, and the calculation of the price:

$$C_{FXP} = (17489 - 371D_p + 2.762D_p^2) \cdot CPI_{2019}$$

Note that CPI_{2019} is equal to 1,1432 (Dec 2022)

The results of all these expressions:

VARIABLE COST		Workhours (h)		Cost (USD)	Cost per aircraft (USD)
Manufacturing	Hmfg	296619,831	Cmfg	20385227,6	81540,91
Quality control			Cqc	2650079,59	10600,32
Total cost of materials			Cmat	296883,01	1187,53
Landing gear			VSC1	0	0
Avionics			VSC2	4473750	17895
Engine			VSC3	759182,5	3036,73
Propeller			VSC4	1456210	5824,84
Battery			VSC5	7500000	30000
Total VSC			Cvsc	14189142,5	56756,57
Variable cost (Only unit.)			Cvar	183835,33	183835,33
Insurance cost			Cins	8437500	33750
Units within 5 years			N	250	NA
Quantity discount factor			Qdf	NA	NA

Table 8.1 Variable costs results.

FIXED COST		Workhours (h)		Cost (USD)	Cost per aircraft (USD)
				3592750,6	
Engineering (92\$/h)	Heng	30116,17	Ceng	8	14371,002
	Htoo		Ctoo	2628648,8	
Tooling (61\$/h)	I	33232,52	I	9	10514,595
Development support			Cdev	292725,08	1170,900
Flight test operations			Cft	219338,01	877,352
				6733462,6	
Total			Cfix	5	26933,850

Table 8.2 Fixed costs results.

The cost distribution can be visualized as follows:

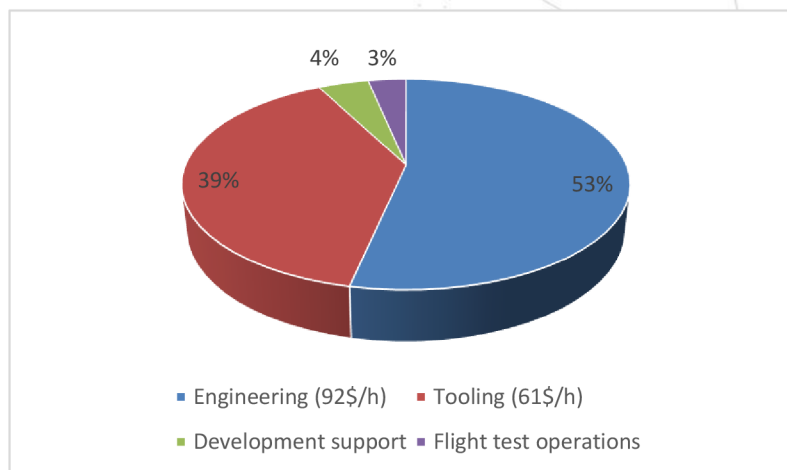


Figure 8.1 Fixed costs distribution.

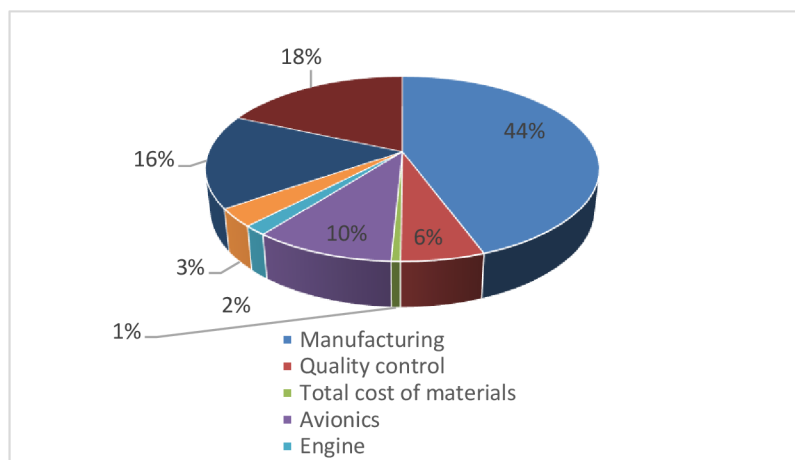


Figure 8.2 Variable costs distribution.

8.3 Aircraft final price and break-even point

After computing both fixed and variable costs, the total cost is obtained by summing these two components. This cost calculation provides us with the minimum selling price required for the aircraft. However, since our objective is to generate revenue, the retail price will exceed this minimum. The retail price will influence the break-even point, which represents the number of aircraft that need to be sold in order to have profit.

	Cost (USD)	Cost per aircraft (USD)
TOTAL COST (Fixed + Variable)	52692295,34	210769,18
Liability insurance (15%)	7903844,302	33750
Minimum selling price	60596139,65	210769,18
Retail price [usd]	225000	
Break-even point [units]	164	

Table 8.3 Retail price and break-even point.

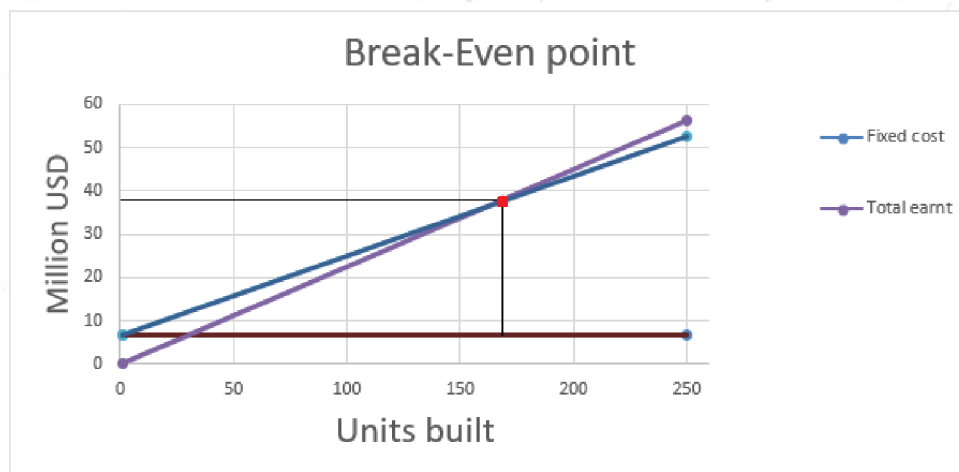


Figure 8.3 Break-even point representation.

Based on our calculations, the minimum recommended retail price for the aircraft is set at \$225,000. At this price point, the break-even point is projected to be 153 units.

9. Result comparison and conclusion.

It should be noted that the results obtained are based on the heaviest setup, and the specifications obtained for the lightest case would provide an improvement in the overall performance. In other words, the results presented refer to the worst-case scenario for the aircraft.

	TARGET	FINAL	VARIATION
MTOW (Kg)	900	1000,4	11%
V_{MAX} (km/h)	295	280	-5,1%
V_{CRUISE}(km/h)	235	220	-6,4%
V_{STALL}(km/h)	>111	95	-14,41%
Range (km)	400	239,4	-40,15%
Endurance (h)	2	1,42	-29%

Table 9.1 Target and computed specifications comparison.

These results reflect the most significant challenge of electric models: range. The energy density of fossil fuels is much higher than of batteries.

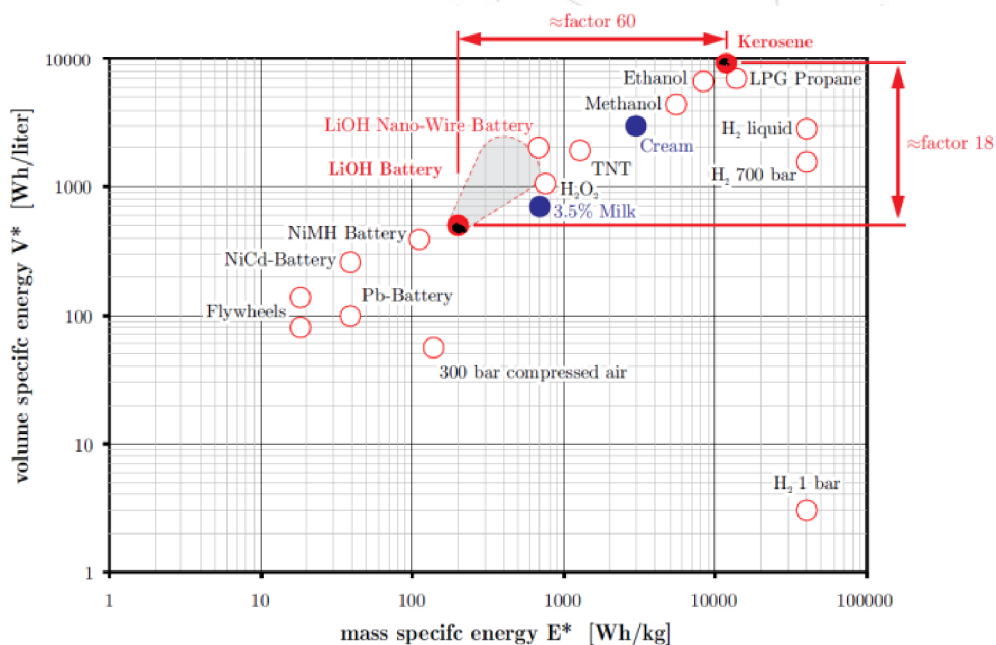


Table 9.2 Gravimetric energy density comparison.

Despite battery technology is improving at an approximate rate of 8% per year, at the current stage of development it is not completely viable to design purely electric aircraft due to the fact that they cannot entirely replace the combustion powered ones. However, the current geopolitical context, coupled with concerns about climate change, has led to increased investments and regulations in favor of green energy and electrification. This is expected to significantly accelerate the development of these technologies and make possible, in the near future, to compare the range and endurance parameters of electric and combustion models.

10. References

- [1] Cessna. (2023, 02 14). *Wikipedia*. Retrieved from https://en.wikipedia.org/wiki/Cessna_152
- [2] Piper Cherokee. (2023, 02 14). Retrieved from Wikipedia: https://en.wikipedia.org/wiki/Piper_PA-28_Cherokee
- [3] Pipistrel. (2023, 02 12). *Pipistrel History*. Retrieved from <https://www.pipistrel-aircraft.com/about-us/history/>
- [4] Wikipedia. (2023). *Bye Aerospace*. Retrieved from https://en.wikipedia.org/wiki/Bye_Aerospace
- [5] Yuneec. (2023). Retrieved from <https://us.yuneec.com/>
- [6] Gudmundsson, S. (n.d.). General Aviation Aircraft Design. In S. Gudmundsson, *General Aviation Aircraft Design - Applied Methods and Procedures (2nd Edition)*.
- [7] EASA. (2023). *CS 23 specs*. Retrieved from <https://www.easa.europa.eu/en/certification-specifications/cs-23-normal-utility-aerobatic-and-commuter-aeroplanes>
- [8] Badis, A. (2017). Subsonic Aircraft Wing Conceptual Design Synthesis and Analysis.
- [9] NASA. (1980). *Technical paper 1786*.
- [10] *Flight Study*. (n.d.). Retrieved from <https://www.flight-study.com/2021/01/effect-of-wing-planform.htm>
- [11] EMRAX. (n.d.). EMRAX 228. Retrieved from <https://emrax.com/e-motors>
- [12] factor, T. I. (2023). Munro 4680 Energy Density Tested.
- [13] epsenergy. (n.d.). *epsenergy*. Retrieved from <https://epsenergy.com/solutions/epic-ultra/>
- [14] Clavero, D. (n.d.). *Diariomotor*. Retrieved from <https://www.diariomotor.com/electricos/movilidad/precios-tarifas-recarga-coche-electrico-puntos-publicos/>
- [15] Roskam, J. (1987). Airplane design Part VI. In J. Roskam.
- [16] Benson, T. (n.d.). NASA.
- [17] Wood, A. (2018). *Aircraft Horizontal and Vertical Tail Design*. Retrieved from <https://aerotoobox.com/design-aircraft-tail/>
- [18] Zikmund, P. (2022). Flight Mechanics I.
- [19] Hlinka, J. (2022). On-board systems I.
- [20] Ferrier, L. (2015). Retrieved from <https://lochief.wordpress.com/2015/08/04/how-the-musk-electric-jet-works/>

- [21] MIT. (n.d.). Retrieved from <https://web.mit.edu/16.unified/www/FALL/thermodynamics/notes/node99.html>
- [22] Han, Z.-H. (2009). *Flight performance analysis of Hybrid Airship*. Retrieved from https://www.researchgate.net/publication/269062335_Flight_Performance_Analysis_of_Hybrid_Airship
- [23] Dineroeneltiempo. (2023). Retrieved from <https://www.dineroeneltiempo.com/dolar/de-2012-a-valor-presente?valor=100&ano2=2023>
- [24] PacificCoastAvionics. (n.d.). Retrieved from <https://www.pacificcoastavionics.com/products/evolution-1500-package?variant=41065152708758>

11. List of parameters

Stall speed	$V_{STALL\ MAX}$	[km/h,m/s,knots]
Cruise speed	V_{CRUISE}	[km/h,m/s,knots]
Air density	ρ	[kg/m ³]
List coefficient	Cl	[-]
Gravity	g	[m/s ²]
Mean aerodynamic chord	C_{mac}	[m]
Diameter of propeller	D_p	[cm]
Max power of the engine	P_{max}	[kW]
Ultimate load factor	nz	[-]
Maximum takeoff weight	MTOW	[kg,lbs]
Wing area	S_w	[ft ²]
Aspect ratio	AR	[-]
Wing weight	W_w	[lbs]
HT area	S	[ft ²]
HT aspect ratio	AR	[-]
Max root chord thickness	t	[ft]
HT Weight	W_{ht}	[lbs]
Thickness	tvt	[ft]
Sweep at 25%	cosA	[-]
VTU weight	W_{vt}	[lbs]
Landing gear weight	W_{lg}	[lbs]
Max power of the engine	P_{max}	[bhp]
Cowling weight	W_{co}	[lbs]
Flight control syst. Weight	W_{ctrl}	[lbs]
Electrical syst. Weight	W_{el}	[lbs]
Furnishing weight	W_{furn}	[lbs]
Gravity center	X_{cg}	[m]
Total weight	W_{tot}	[lbs,kg]

Zero lift drag coefficient	Cdo	[-]
Induced drag coefficient	Cdi	[-]
span efficiency factor	e	[-]
Wing/fus interference factor	Rwf	[-]
Turbulent flat plate friction coeff	Cffus	[-]
Fuselage length	Lf	[ft]
Aircraft max. Diameter	Df	[ft]
Wetted surface fuselage	Swetfus	[ft ²]
Angle of attack	AoA	[deg,grad]
Fus Zero lift drag coeff	Cdofus	[-]
fuselage Induced drag coeff	Cdifus	[-]
Wing/fuselage interference factor	Rwf	[-]
Max thickness location coeff	L'	[ft]
Max thickness ratio	t/c	[-]
Power available	Pavailable	[kW]
Power required	Preq	[kW]
Flight altitude	H	[km]
Power excess	Pexcess	[kW]
Rate of climb	-	[m/s]
Range	R	[km]
Battery mass	M_batt	[kg]
Aircraft mass	Maircraft	[kg]
takeoff airborne distance	Sa	[m]
takeoff ground distance	Sg	[m]
Weight airframe	Wairframe	[lbs]
Max level airspeed	Vh	[KTAS]
Planned production	N	[uds]
Certification factor	Fcert	[-]
Fcf1		[-]
Complexity factor	Fcomp	[-]
Pressurization factor	Fpress	[-]

Engineering Hours	Heng	[hrs]
Max level airspeed	Vh	[KTAS]
Planned production	N	[uds]
Estimated prod. rate	Qm	[uds]
Tooling hours	Htooling	[hrs]
Manufacturing labor hours	Hmfg	[hrs]
Engineering rate	Reng	[\$/h]
Consumer price index	CPI012	[-]
Engineering cost	Ceng	[USD]
Number of prototypes	N	[uds]
Development support costs	Cdev	[USD]
Flight test operations	Cft	[USD]
Tooling rate	Rtool	[USD/h]
Tooling cost	Ctool	[USD]
Manufacturing rate	Rmfg	[USD/h]
Manufacturing cost	Cmfg	[USD]
Cost of materials	Cmat	[USD]
